ผลของลำดับในการเติมโลหะทรานซิชันและแมกนีเซียมที่มีต่อปฏิกิริยาการเผาไหม้พาทาลิก

แอนไฮไดรด์บนตัวเร่งปฏิกิริยาออกไซด์ของโลหะทรานซิชันที่สนับสนุนด้วยแมกนีเซียมออกไซด์

นางสาวสุธีรา น่วมพิทักษ์

EFFECTS OF TRANSITION METAL AND MAGNESIUM LOADING SEQUENCE ON THE COMBUSTION OF PHTHALIC ANHYDRIDE OVER MgO PROMOTED TRANSITION METAL OXIDE CATALYSTS

Miss Suteera Nuampituk

Thesis Title   EFFECTS OF TRANSITION METAL AND MAGNESIUM LOADING SEQUENCE ON THE COMBUSTION OF PHTHALIC ANHYDRIDE OVER MgO PROMOTED TRANSITION METAL OXIDE CATALYSTS

By   Miss Suteera Nuampituk

Field of Study Chemical Engineering

Thesis Advisor Associate Professor Tharathon Mongkhonsi, Ph.D.

_____

Accepted by the Faculty of Engineering, Chulalongkorn University in Partial Fulfillment of Requirements for the Master's Degree

........…………………………….Dean of Faculty of Engineering

(Professor Somsak Panyakeow, D.Eng.)

THESIS COMMITTEE

....Chairman

(Associate Professor Suttichai Assabumrungrat, Ph.D.)

....Thesis Advisor

(Associate Professor Tharathon Mongkhonsi, Ph.D.)

.... Member

(Assistant Professor M.L.Supakanok Thongyai, Ph.D.)

....Member

(Joongjai Panpranot, Ph.D.)

สุธีรา   น่วมพิทักษ์ : ผลของลำดับในการเติมโลหะทรานซิชันและแมกนีเซียมที่มีต่อ
ปฏิกิริยาการเผาไหม้พาทาลิกแอนไฮไดรค์บนตัวเร่งปฏิกิริยาออกไซด์ของโลหะทรานซิชัน
ที่สนับสนุนด้วยแมกนีเซียมออกไซด์ (EFFECTS OF TRANSITION METAL AND
MAGNESIUM LOADING SEQUENCE ON THE COMBUSTION OF PHTHALIC
ANHYDRIDE OVER MgO PROMOTED TRANSITION METAL OXIDE
CATALYSTS)
อ. ที่ปรึกษา : รศ. ดร. ธราธร มงคลศรี, 90 หน้า. ISBN 974-17-2050-5

การศึกษาสมบัติออกซิเดชันของตัวเร่งปฏิกิริยาโครเมียม แมงกานีส โมลิบดีนัม ทังสเตน
เหล็ก สังกะสี ที่ได้รับการสนับสนุนด้วยแมกนีเซียมออกไซด์บนตัวรองรับอลูมินา โดยใช้ปฏิกิริยา
การเผาไหม้ของสารประกอบพาทาลิกแอนไฮไดรค์ ผลการทดลองแสดงให้เห็นว่าลำดับการเติม
โลหะทรานซิชันและแมกนีเซียม มีผลกระทบต่อความว่องไวในการทำปฏิกิริยาของตัวเร่งปฏิกิริยา
โดยไปเปลี่ยนจำนวนตำแหน่งที่เป็นเบสให้มากขึ้นหรือลดลง ซึ่งการมากขึ้นหรือลดลงของตำแหน่ง
ที่เป็นเบสบนพื้นผิวจะให้ผลเป็นไปในทางบวกหรือทางลบขึ้นอยู่กับชนิดของโลหะทรานซิชันและ
ปริมาณแมกนีเซียมที่เลือกใช้   ถ้าปริมาณแมกนีเซียมที่เลือกนั้นน้อยกว่าค่าเหมาะสม วิธีการ
เตรียมที่ทำให้ตำแหน่งที่เป็นเบสบนพื้นผิวมีปริมาณเพิ่มขึ้นจะทำให้ความว่องไวเพิ่มขึ้น แต่ถ้า
แมกนีเซียมที่เลือกมามากกว่าปริมาณที่เหมาะสม วิธีการเตรียมที่ทำให้ตำแหน่งที่เป็นเบสบนพื้น
ผิวมีปริมาณมากขึ้น จะทำให้ความว่องไวของตัวเร่งปฏิกิริยาลดลง

ภาควิชา......วิศวกรรมเคมี..............   ลายมือชื่อนิสิต…………………………..
สาขาวิชา......วิศวกรรมเคมี………….   ลายมือชื่ออาจารย์ที่ปรึกษา…………………
ปีการศึกษา......**2545**………………

SUTEERA NUAMPITUK : EFFECTS OF TRANSITION METAL AND MAGNESIUM LOADING SEQUENCE ON THE COMBUSTION OF PHTHALIC ANHYDRIDE OVER MgO PROMOTED TRANSITION METAL OXIDE CATALYSTS.

THESIS ADVISOR: ASSOC.PROF. THARATHON MONGKHONSI, Ph.D. 90 pp. ISBN 974-17-2050-5.

The oxidation property of the Cr, Mn, Mo, W, Fe and Zn promoted MgO on Al_2O_3 supported catalysts on the combustion of phthalic anhydride were investigated. It was found that the loading sequence of the metal affected the catalytic activity by changing the number of the surface basic sites. The effects would be positive or negative depended on the type of transition metal and the amount of the magnesium selected. If the amount of magnesium selected was lower than the optimum amount, the procedure that resulted in a larger number of the surface basic site would yield a catalyst with higher catalytic activity. On the other hand, if the amount of magnesium selected was higher than the optimum amount, the procedure that resulted in a larger number of the surface basicity would decrease the catalytic activity.

Department …Chemical Engineering… Student's signature…………………………..

Field of study... Chemical Engineering ... Advisor's signature……………………………

Academic year…………2002……………….

ACKNOWLEDGEMENTS

The author would like to express her greatest gratitude to her advisor, Associate Professor Tharathon Mongkhonsi, for his invaluable guidance throughout this study. Special thanks to Professor Dr. Piyasan Praserthdam for his kind supervision of this research. In addition, I would also grateful to Associate Professor Suttichai Assabumrungrat, as the chairman, Assistant Professor Supakanok Thongyai and Dr. Joongjai Panpranot, member of thesis committee.

Many thanks for his kind suggestions and useful help to Mr. Veerawat Manomaiviboon, Miss Jittigan Nugoolchit, Miss Khanitta Thammajariyawongsa and many best friends in Chemical Engineering department who have provided encouragement and cooperation throughout this study.

Finally, she also would like to dedicate this thesis to her parents who have always been the source of her support and encouragement.

CONTENTS

CONTENTS (Cont.)

LIST OF TABLES

LIST OF FIGURES

LIST OF FIGURES (Cont.)

CHAPTER I

INTRODUCTION

In the manufacture of organic chemicals, oxygen may be incorporated into the final product, as in the oxidation of propylene to acrolein or *o*-xylene to phthalic anhydride; or the reaction may be an oxidative dehydrogenation in which the oxygen does not appear in the desired product, as in the conversion of butylene to butadiene. The desired reaction may or may not involve C-C bond scission.

Complete catalytic oxidation is a practicable method for elimination of organic pollutants in gaseous streams. Direct oxidation of alkanes and aromatic compounds is an important process in petrochemical industry. The partial oxidation reaction can be carried out in either gaseous or liquid phase depended on the thermal stability of the product formed. Usually, the gas phase oxidation is more preferred since the process has lower hydrocarbon inventory than the liquid phase oxidation.

Examples of gas phase oxidation process are the oxidation of o-xylene to phthalic anhydride and benzene to maleic anhydride. In both processes, the aromatic reactants are vapourised and mixed with air in gaseous phase. The concentration of the aromatic is limited by the lower explosive limits of the gas mixture. The gas mixture then flows to a reactor containing several thousands of catalyst tubes. The products formed, the anhydrides, are recovered by cooling the product gas stream using a condenser.

At the condenser, it is known that the lower coolant temperature, the higher product recovery. In practice, the temperature at the condenser is limited by the concentration of water in the product gas stream. If water is allowed to condense, corrosion will occur. The effluent gas leaving the condenser, therefore, still contains traces of organic compounds including the hydrocarbon reactant and the anhydride product.

Eliminating the remaining organic compounds from the effluent gas is necessary. At present, the removal can be carried out by sending the effluent gas, which still contains high oxygen concentration to a furnace or a boiler. This method, however, may cause problem concerning the energy balance of the plant and NO_x forming from high temperature combustion. Catalytic combustion is an alternative. There are two catalyst families which can completely oxidise organic compounds. One is the Pt-based catalysts and the other one is the acidic oxide based catalysts.

The Pt-based catalysts can initiate the combustion of the organic compounds at a lower temperature than the acidic metal oxide-based catalysts, typically 100-200° C lower. But the Pt-based catalysts can not withstand prolong operation in a high oxygen concentration atmosphere. The acidic metal oxide-based catalysts work better in the latter case.

An important nature of the acidic metal oxide catalyst is its capability to adsorbed acidic organic compounds. On the acidic surface, the acidic organic compounds are less likely to be adsorbed. The further oxidation of the acidic compound to combustion products, therefore, is low. Because of this reason, the acidic metal oxide catalyst becomes a selective oxidation catalyst for the production of anhydrides because it has low ability to further oxidise the anhydride products formed. On the contrary, this behaviour causes problem when one has to use it as a combustion catalyst.

In order to overcome the aforementioned problem, we propose to dope a basic metal oxide compound to an acidic metal oxide catalyst to enhance the adsorption of the acidic organic compounds. However, the consideration of basic metal oxide is an important. Too strong basic metal oxide cause the catalyst adsorbed carbon dioxide leading to carbonate compound formed which deactivated the catalyst. But too weak basic metal oxide led to insufficient ability to adsorb organic acid of the catalyst.

Magnesium oxide is a suitable basic metal oxide because it is not too strong basic metal oxide until adsorbed carbon dioxide to form carbonate compound. But it is strong enough to adsorbed organic acids [Kanokrattana (1997), Ali et al.(2000)].

In a concurrent research, it is demonstrated that some supported acidic (Cr, Mn, Mo and W) and amphoteric (Fe and Zn) transition metal oxides doped with MgO at an appropriate amounts have higher phthalic anhydride combustion activity than the base oxide catalysts. In that research, the transition metals and magnesium were co-impregnated on to the support, Al_2O_3. The co-impregnation technique, though has fewer preparation steps than the sequential impregnation technique, may not yield a best active compound. When two metal are impregnated on the same support, they may form separate oxides of each own or a new mixed oxide compound. The final oxide compound depends on the nature of the metals and the preparation technique.

For example, effects of transition metal and magnesium loading sequence when two metals are impregnated on support, the sequence of metal loading can affect the structure and/or activity of the final catalyst obtained. A catalyst with two metals A and B may be prepared using co-impregnation or sequential impregnation methods. The co-impregnation method begins by dissolving salts of both metals in a solvent containing a catalyst support. Then, the solvent is vaporized to allow the metals to deposit on the support surface. The solid obtained (A-B/support) is dried and calcined to transform the deposited metals into oxide forms. During the calcinations step, both metals may form separate metal oxide compounds (A-oxide, B-oxide/support) or a new complex oxide composed of cation of both metals (A-B-oxide/support).

The sequential impregnation process begins by depositing only one metal (metal A) on the support first. The solid obtained (A/support) is calcined to change the salt of metal A to an A-oxide compound (A-oxide/support). The A-oxide/support is subsequently impregnated with the second metal. The solid obtained from the second impregnation step contains metal A in the form of oxide and metal B in the form of a salt (A-oxide, B/support). The "A-oxide, B-support" is further calcined to change the salt of metal B into an oxide form. If the A-oxide can withstand the conditions used in the second calcinations step, then the A-oxide will not react with the salt of metal B, leaving metal B to form a separate metal oxide. The catalyst obtained will contain the oxides of metal A and B (A-oxide, B-oxide/support). If the A-oxide cannot withstand the conditions used in the second calcinations step, then the A-oxide may fuse with the salt of metal B and form a new A-B-oxide system. The

catalyst obtained will contain a complex oxide composed of metals A and B (A-B-oxide/support) [Mongkhonsi (2002)].

In this research chromium-magnesium oxide, molybdenum-magnesium oxide, tungsten-magnesium oxide, manganese-magnesium oxide, iron oxide and zinc oxide supported on Al_2O_3 is used as catalyst for combustion of phthalic anhydride.

In this study the effects of sequence of transition metal and magnesium loading of Cr-Mg-O/Al_2O_3, Mn-Mg-O/Al_2O_3, Mo-Mg-O/Al_2O_3, W-Mg-O/Al_2O_3, Fe-Mg-O/Al_2O_3, Zn-Mg-O/Al_2O_3 catalysts have been used to investigate:

1. The oxidation property of Cr-Mg-O/Al_2O_3, Mn-Mg-O/Al_2O_3, Mo-Mg-O/Al_2O_3, W-Mg-O/Al_2O_3, Fe-Mg-O/Al_2O_3, Zn-Mg-O/Al_2O_3 catalysts for phthalic anhydride reactant.
2. The effects of transition metal and magnesium loading sequence on the combustion of phthalic anhydride over MgO promoted transition metal oxide catalysts.

This present work is organized as follows:

Chapter II contains literature reviews of chromium oxide, molybdenum oxide, tungsten oxide, manganese oxide, iron oxide, zinc oxide and supported catalysts on various reactions

The theory of this research, studies about the oxidation reaction and its possible mechanism, reaction of anhydrides, properties of chromium oxide, molybdenum oxide, tungsten oxide, manganese oxide, iron oxide, zinc oxide and supports are presented in chapter III.

Description of experimental systems and the operational procedures are described in chapter IV.

Chapter V reveals the experimental results of the characterization of Cr-Mg-O/Al_2O_3, Mn-Mg-O/Al_2O_3, Mo-Mg-O/Al_2O_3, W-Mg-O/Al_2O_3, Fe-Mg-O/Al_2O_3, Zn-Mg-O/Al_2O_3 catalysts and the oxidation reaction of phthalic anhydride over these catalysts.

Chapter VI contains the overall conclusion emerged from this research.

Finally, the sample of calculation of catalyst preparation, external and internal diffusion limitations, calibration curves from area to mole of phthalic anhydride and data of this experiment which has emerged from this study are included in appendices at the end of this thesis.
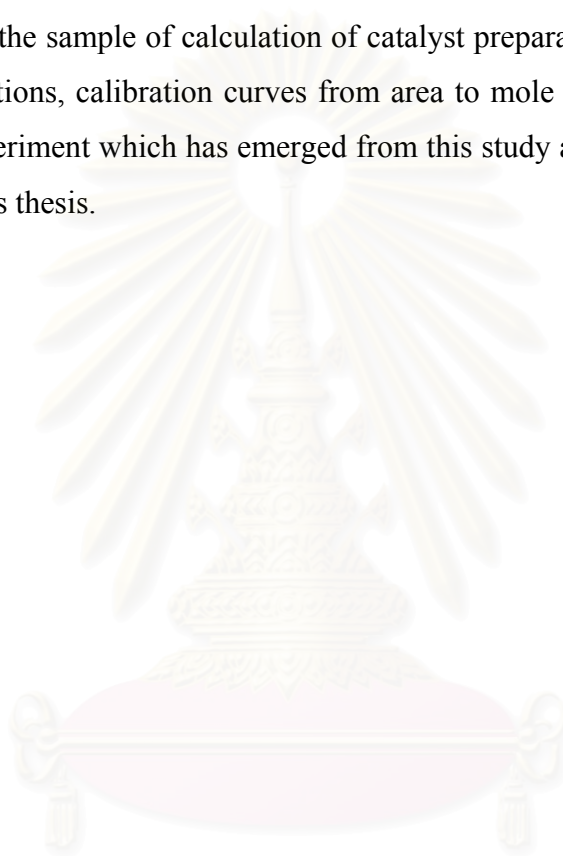
CHAPTER II

LITERATURE REVIEW

The heterogeneous catalytic oxidation on transition metal oxides was extensively used in catalysis for selective and total oxidation process. The complete catalytic oxidation was widely used method for elimination of organic pollutants in gaseous streams to CO_2 and water. A large body of literature was concerned with the development of catalysis for this reaction. For many researches, transition metal oxide catalysts can completely oxidise organic compounds.

This chapter reviews the works about the combustion of phthalic anhydride on Co-Mg-O/Al_2O_3 and V-Mg-O/TiO_2, the processes for recovery of phthalic anhydride, the treatment of byproducts obtained in the preparation of phthalic anhydride, the transition metal oxide and supported transition metal oxide catalysts in the various reactions.

2.1 Literature reviews

Toyada and Teraji (1980) invented a process that allows the treatment of byproducts obtained in the preparation of phthalic anhydride without creating secondary pollution. Byproducts were treated by heating the byproducts to a temperature sufficient to maintain the byproducts in a molten state and thereafter atomizing air having a temperature of at 60°C for combustion. The byproducts may be low boiling point and/or high boiling point fractions obtained in the purification step by distillation of crude phthalic anhydride produced by the partial oxidation of ortho-xylene or naphthalene.

Keuneche *et al.* (1981) invented a process for continuously separating phthalic anhydride from the reaction gases of the catalytic oxidation of o-xylene and/or naphthalene by treating reaction gas mixture with a maleic anhydride absorbent. Even though pure maleic anhydride could be used as an absorbent, maleic anhydride containing phthalic anhydride was usually used so as to keep the costs of regenerating

the absorbent within economical bounds. Thus, maleic anhydride could contain up to 85% by weight phthalic anhydride. Absorption could be performed in two or more stages, preferably in two stages. The reaction gas, with a temperature from 135 - 150° C, was introduced into the absorption zone, and withdrawn at a temperature from 45 - 80°C from the absorption zone. The maleic anhydride, which was loaded with phthalic anhydride, was separated through distillation into raw phthalic anhydride as a bottoms product and an overhead product primarily containing maleic anhydride. The overhead product was then returned into the absorption zone. The raw phthalic anhydride was treatment and then purified through distillation, e.g. in a continuous, two stage distillation in which light, volatile impurities, such as residual maleic anhydride and benzoic acid, were distilled off in the first stage and the pure phthalic anhydride was distilled in the second as an overhead product. The gas leaving the absorption zone and containing small amounts of maleic anhydride was scrubbed with water. The maleic acid solution recovered from this scrubbing was evaporated, the maleic acid was dehydrated and distilled, and a part of the maleic anhydride distillate was returned into the absorption zone.

Way and Peter (1981) invented an apparatus for recovery of vaporized phthalic anhydride from the gas streams. Phthalic anhydride was recovered from gases in a multiple heat-pipe exchanger system, one or more for condensing phthalic anhydride from gases containing vapors thereof and one or more simultaneously melting out the condensed phthalic anhydride solids. The exchangers being switched in alternate cycles to melt out from the surfaces of the exchanger tube ends on which the phthalic anhydride solids were first accumulated, and to condense phthalic anhydride solids in the exchanger from which the phthalic anhydride was cleared by melting out. The cooling to recover phthalic anhydride was economical and efficient with ambient air, and the heating to melt out accumulated phthalic anhydride was effected with hot gases, such as combustion gases, preferably by incineration of residual phthalic anhydride tail gas from which phthalic anhydride was condensed, or other hot combustion gases, but other sources of heating the air or gases may be optionally substituted.

McCabe and Mitchell (1983) studied the oxidation of ethanol and acetaldehyde over alumina supported catalysts. Pt/Al_2O_3 catalysts were only slightly more active than metal oxide catalysts for the same volume in the combustion of ethanol.

Spivey (1987) reviewed the complete catalytic oxidation of volatile organics. Both metal oxides and supported noble metals are active for many deep oxidations. (The mechanism of deep catalytic oxidation involves both lattice and surface oxygen for metal oxides and probably reduced metal sites for supported noble metals.) Metal oxide catalysts were generally less active than were supported noble metals, but the were somewhat more resistant to poisoning. This poison resistance may be due to the high active surface area of metal oxides compared to supported noble metals. The most active single metal oxide catalysts for complete oxidation for a variety of oxidation reactions were usually found to be oxides of V, Cr, Mn, Fe, Co, Ni and Cu. The mechanism of oxidation on these oxide catalysts was generally thought to involve strong adsorption of the organic compound at an anionic oxygen site in the oxide lattice leading to the formation of an activated complex. This complex could then react further to yield products of complete combustion.

Ozkan et al. (1990) investigated the methanol oxidation over nonprecious transition metal oxide catalysts. Catalytic oxidation of methanol over a series of first row transition metal oxide catalysts (Cr, Mn, Fe, Co, Ni, Cu). All catalysts exhibited similar activities for methanol conversion, but the supported copper catalyst was found to be considerably more selective to CO_2.

Hess et al. (1993) studied the catalyst containing metal oxides for use in the degenerative oxidation of organic compounds present in exhaust gases from combustion plants. A metal oxide containing catalysts which contained oxides of titanium and/or zirconium, oxides of vanadium and/or niobium and oxides of molybdenum, tungsten, and chromium. It was found that the adding of alkaline earth metal sulfates produced a catalyst, which was clearly superior to catalysts composed only of the metal oxides. The catalyst preferably contained the following

components: titanium dioxide, especially in the form of anatase, vanadium oxide in the form of V_2O_5 and tungsten oxide in the form of WO_3.

Kang and Wan (1994) studied the effects of acid or base additives on the catalytic combustion activity of chromium and cobalt oxides. It was found that the base additive could enhance the catalytic activity of Cr, Co/Al_2O_3 for carbon monoxide oxidation, but the acid additive reduces the activity. For ethane combustion, the addition of a base additive to the catalyst could reduce the ethane conversion. The selectivity of carbon dioxide, however, was increased to 100% because the rate of carbon monoxide oxidation was enhanced. On the other hand, the addition of acid additive to the catalyst gave an increase in ethane conversion, but the selectivity to carbon dioxide was reduced.

Leklertsunthon (1998) investigated the oxidation property of a series of V-Mg-O/TiO_2 catalyst in the oxidation reaction of propane, propene, 1-propanol and carbon monoxide. It had been found that the catalytic behavior of the catalyst depended on the reactants. Propene and CO_2 were the major products in the propane oxidation reaction. The vanadium and magnesium contents affected the catalytic property of the V-Mg-O/TiO_2 catalyst in the reaction. The sequence of magnesium loading also affected the structure and catalytic performance of this catalyst. In addition, this catalyst was inactive for propene oxidation, from which it could be indicated that propene formed in propane oxidation reaction was not further oxidized to CO_2. According to 1-propanol oxidation, propionaldehyde was the main observable product at low reaction temperatures, and it was oxidized rapidly to CO_2 when the reaction temperature was increased. Moreover, the dehydration of 1-propanol became significant at high temperatures. It was found that the sequence of magnesium loading and magnesium content had no effect on the catalytic performance of the catalyst. On the other hand, increasing vanadium content improved the propene selectivity and decreased the CO_2 selectivity. Finally, in CO oxidation, this catalyst was rather inactive. Since CO was an unobservable product in propane, propene and 1-propanol reactions, on the V-Mg-O/TiO_2 catalysts, CO was not produced in these three reactions.

McCarty *et al.* (1999) investigated the stability of supported metal and supported metal oxide combustion catalysts. Durable catalysts must be able to resist the loss by vaporization. This property limited the use of noble metal and single-phase transition metal oxides as catalysts. The transition metal oxides had high volatility at high temperatures (>1000 °C). Incorporation of transition metal oxides into complexes with materials such as alumina could lower their volatility by factors from 10 to 1000. The most stable catalytically active materials appeared to be Pd and Fe_2O_3 and use of these materials was recommended for long-term use in high temperature combustors.

Chaiyasit (2000) investigated the selective oxidation reaction of 1-propanol and 2-propanol over Co-Mg-O/TiO_2 (8wt%Co, 1wt%Mg) catalyst. It was found that the oxidation property of Co-Mg-O/TiO_2 catalyst depends on type of the reactants. Propionaldehyde is the main product for selective oxidation of 1-propanol. In case of 2-propanol oxidation reaction, it is found that Co-Mg-O/TiO_2 catalyst is an active catalyst for selective oxidation reaction. The main product at low reaction temperature is propylene while at high reaction temperature the main reaction products are propylene and propionaldehyde. From the result of propylene oxidation, it can be indicated that propionaldehyde is produced directly from propylene. In addition, the sequence of cobalt and magnesium loading has no effect on the structure and catalytic performance of this catalyst. While the type of support affects the selectivity of supported cobalt catalyst.

Larsson and Andersson (2000) studied the oxides of copper, ceria promoted copper, manganese and copper manganese on Al_2O_3 for the combustion of CO, ethyl acetate and ethanol. The $CuMn_2O_4$/Al_2O_3 catalyst was more active than the CuO_x/Al_2O_3 and Mn_2O_3/Al_2O_3 catalyst for the complete oxidation of CO, ethyl acetate and ethanol. The characterization with XRD indicated that the copper oxide was presented as a copper aluminate surface phase on alumina with low copper oxide loading. At high loading, bulk CuO crystalites were presented as well. The active metal oxides in the alumina supported copper manganese oxide and manganese oxide catalysts were mainly presented as crystalline $CuMn_2O_4$ and Mn_2O_3, respectively.

Tongsang (2001) reported the oxidation property of the V-Mg-O/TiO$_2$ catalysts on the combustion of phthalic anhydride and maleic anhydride is investigated. From the results, the MgO modified V$_2$O$_5$/TiO$_2$ catalysts can better oxidize the anhydride ring than the unmodified one. Additionally, the appropriate ratios of vanadium per magnesium lead to a balance between the adsorption of the anhydrides and the catalytic activity of vanadium and titania support.

Umpo (2001) investigated the oxidation property of the Co-Mg-O/Al$_2$O$_3$ catalyst on the combustion of phthalic anhydride and maleic anhydride. The results show that magnesium promotes the adsorption of anhydride leading to better combustion of the anhydrides. The research also found that the ratio of cobalt per magnesium should be at an appropriate ratio to keep a balance between the adsorption of the anhydrides and the catalytic activity of cobalt and alumina support.

Cherian *et al.* (2002) studied the oxidative dehydrogenation of propane over Cr$_2$O$_3$/Al$_2$O$_3$ and Cr$_2$O$_3$ catalysts. It was found that bulk Cr$_2$O$_3$ was efficient for complete combustion. However, when Chromia was supported on another metal oxide (e.g. Al$_2$O$_3$, TiO$_2$, SiO$_2$, ZrO$_2$, etc.), the structure and reactivity properties were altered. The characterization with XRD indicated that all the Cr$_2$O$_3$/Al$_2$O$_3$ samples had the major peaks at 46.1 and 67.8° with and additional broad peak between 36 and 38°. These peaks were due to the γ-Al$_2$O$_3$ support. For the 20% Cr$_2$O$_3$/Al$_2$O$_3$ sample, the additional peaks to peaks due to Cr$_2$O$_3$ crystals. Thus, from the XRD it appeared that the monolayer coverage was exceeded for 20% Cr$_2$O$_3$/Al$_2$O$_3$ sample.

Liu *et al.* (2002) studied the diesel soot oxidation with NO$_2$ and O$_2$ on supported metal oxide catalyst. Among the single oxide catalysts supported on SiO$_2$, oxides with relatively low melting points or high vapor pressures, such as Re$_2$O$_7$, MoO$_3$ and V$_2$O$_5$ showed high activities. MoO$_3$/SiO$_2$ was the most active catalysts among the MoO$_3$/support catalysts. Combination of MoO$_3$ with Fe$_2$O$_3$ and Co$_3$O$_4$ deteriorated catalytic performance, whereas, combination of CuO with MoO$_3$ or V$_2$O$_5$ promoted oxidation of carbon at high temperatures.

Paola *et al.* (2002) studied the catalytic photo oxidation reactions with aliphatic and aromatic organic compounds having different acid strengths. The catalysts are TiO_2 powders doped with various transition metal ions (Co, Cr, Cu, Fe, Mo, V and W). The co-doped powder showed to be more photoactive than the bare TiO_2 for methanoic acid degradation while the behavior of TiO_2/Cu and TiO_2/Fe was similar to that of the support. TiO_2/W was the most efficient sample for the photo degradation of benzoic acid and 4-nitrophenol, TiO_2 the most active powder for ethanoic acid.

2.2 Comment on previous works

From the above reviewed literature, it can be seen that transition metal oxides show the high activity of oxidation the organic compounds. However, there is no information about the effect of transition metal and magnesium loading sequence on the combustion of phthalic anhydride over MgO promoted transition metal oxide catalysts. In the concurrent research, it is toward that some supported acidic transition metal oxides (Cr, Mn, Mo and W) and some amphoteric transition metal oxides (Fe and Zn) promoted with MgO show higher phthalic anhydride combustion activity than the base oxide. In this research, the system consists of transition metal oxide (Cr, Mn, Mo, W, Fe and Zn), Al_2O_3 and MgO to study the catalytic property in the combustion anhydride.

CHAPTER III

THEORY

Catalytic oxidation can be categorized as complete oxidation and selective oxidation. Complete oxidation is the combustion of organic compound to the combustion products; CO_2 and H_2O [Thammanonkul (1996)]. It is a practicable method for elimination of organic pollutants in gaseous streams. While selective oxidation is the reaction between hydrocarbon and oxygen to produce oxygenates (such as alcohols, aldehydes, carboxylic acids which are produced from partial oxidation processes) or unsaturated hydrocarbons (such as ethane and propene which can be produced from oxidative dehydrogenation process) [Thammanonkul (1996)].

In studies on oxidative catalysis; commonly great attention is attached to the state of oxygen on the catalyst surface. A relative inert oxygen molecule is activated by interacting with the surface of oxide catalyst. The main parameter determining oxygen reactivity on the catalyst is energy of oxygen binding with the catalyst as a thermochemical characteristic. Correlation between rates of catalytic oxidation and oxygen binding energy on oxide catalysts have been established. The weaker the oxygen binding with the catalyst surface, the more efficient is complete oxidation with this catalyst [Satterfield (1991)].

With oxide catalysts, chemisorbed surface oxygen as well as lattice oxygen may play a role. The oxidation of propylene to acrolein on a $BiMo/SiO_2$ catalyst in a pulsed reactor showed by isotopic oxygen studies that surface chemisorbed oxygen as well as lattice oxygen could contribute to the overall reaction. It seem plausible that in many other cases chemisorbed oxygen would lead to a different set of products than lattice oxygen and both mechanisms could be significant. On the basis of other studies advanced the hypothesis that surface-adsorbed oxygen may in general lead to products of complete oxidation and the lattice oxygen is needed for partially oxidized products, but more study is need to test this proposal [Satterfield (1991)].

3.1 Mechanism of oxidation reaction

The mechanisms of oxidation reaction on the catalyst surface was shown as follow:

Reaction between reactant and adsorbed surface oxygen species,

Reactant (fluid phase) $\rightarrow$ Reactant (surface species)

Oxygen (fluid phase) $\rightarrow$ Oxygen (surface species)

Reactant (surface species) + Oxygen (surface species) $\rightarrow$ Product (surface species)

Product (surface species) $\rightarrow$ Product (fluid phase)
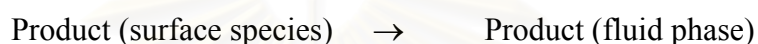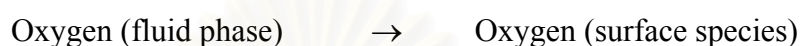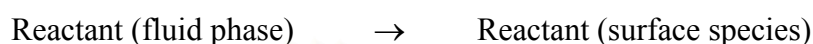
3.2 Magnesium promoted transition metal oxide catalyst

Transition metal oxides were interesting materials in the field of heterogeneous catalysis. The most active single metal oxide catalysts for complete oxidation for a variety of oxidation reactions were usually found to be oxides of V, Cr, Mn, Fe, Co, Ni, and Cu. For the complete oxidation of methane, methanol, ethanol, acetaldehyde, and ethanol/methanol mixture, the transition metal oxide catalysts exhibited high activity, but the most active catalyst was copper oxide catalyst. This was followed by chromium oxide catalyst. The $CuMn_2O_4/Al_2O_3$ catalyst was more active than the CuO_x/Al_2O_3 and Mn_2O_3/Al_2O_3 catalyst for the complete oxidation of CO, ethyl acetate, and ethanol. For the oxidative dehydrogenation of propane, the Cr_2O_3 catalyst was efficient for complete combustion. The MoO_3/SiO_2 was the most active catalysts among the $MoO_3/support$ catalysts for the diesel soot oxidation. For the photo-oxidation of benzoic acid and 4-nitrophenol, TiO_2/W was the most efficient catalyst.

MgO is white powder that usually obtained by dehydration of magnesium dihydroxide. Its catalytic interest lies in its essentially basic surface character, which makes it an effective catalyst support. Magnesium oxide is also interesting because it has the ability to stabilize metals in unusual oxidation states and to avoid sintering and evaporation of the metal atoms [Aramendia *et al*. (1999)].

3.3 Acidic and Basic Catalyst [Kirk-Othmer (1979)]

The correlation of catalytic efficiency with the strength of the acid or base is of considerable importance. The general theory of acid-base catalysis in which a proton is transferred from the catalyst to the reactant (acid catalysis) or from the reactant to the catalyst (base catalysis). The velocity of the catalyzed change is thought to be determined by a protolytic reaction between the reactant and the catalyst. The molecule, on receiving or giving a proton, is converted into an unstable state which immediately (or very rapidly, compared with the velocity of the protolytic reaction) leads to the reaction under consideration. Thus, acid catalysis of a basic reactant is represented by the general scheme $R+AH^+ \rightarrow RH^++A$, whereas $RH^++B \rightarrow R+BH^+$ represents basic catalysis of an acidic reactant.

3.4 Chemisorption at oxide surface [Bond (1987)]

On the basis of their electrical conductivities, solids are traditionally divided into four classes as shown in Table 3.1.

Table 3.1 Classification of solids by electrical conductivity

Class	Conductivity range (Ω cm^{-1})	Chemical class	Examples
Superconductors	up to 10^{35}	metals at low temperatures	-
Conductors	10^4-10^6	metals and alloy	Na, Ni, Cu, Pt etc.
Semiconductors	10^3-10^8	(a) intrinsic: semi-metals	Ge, Si, Ga, As etc.
		(b) extrinsic: oxides and sulphides of transition and post-transition elements	ZnO,Cu$_2$O, NiO, ZnS,MoS$_2$, NiS etc.
Insulators	10^{-9}-10^{-20}	stoichiometric oxides	MgO, SiO$_2$, Al$_2$O$_3$ etc.

There are two classes of semiconductors. Group IV elements such as silicon and germanium, and analogous Group III-Group V compounds like gallium arsenide, are termed *intrinsic* semiconductors because their conductivity is an inherent feature of their chemical structure. However, important as these substances are in solid state devices, they are not catalytically active and will not be considered further. Of greater interest are the oxides and sulphides whose conduction is due to their departure from precise stoichiometry: these substances are termed *extrinsic* or defect semiconductors. The more non-stoichiometric they are, the greater their conductivity. Another important general feature of semiconductors is that their conductivity increases with temperature according to a relation similar to the Arrhenius equation.

A useful generalization concerning the requirement for p-type semi-conductivity is that the cation shall have an accessible higher oxidation state: thus cobalt(II)oxide and copper(I)oxide are also in this group. For n-type semiconductivity an accessible lower oxidation state (which may include the zero-valent state) is needed: thus cadmium oxide and iron(III)oxide fall in this group (see Table 3.2).

Table 3.2 Classification of semiconducting metal oxides

Effect of heating in air	Classification	Examples
Oxygen lost	Negative (n-type)	ZnO, Fe_2O_3, TiO_2, CdO, V_2O_5, CrO_3, CuO
Oxygen gained	Positive (p-type)	NiO, CoO, Cu_2O, SnO, PbO, Cr_2O_3

3.5 Chemisorption on semiconducting oxides

A qualitative understanding of the chemisorption of simple gases on semiconducting oxides follows simply from their chemistry. Reducing gases such as hydrogen and carbon monoxide are adsorbed strongly, but irreversibly: on heating, only water and carbondioxide respectively can be recovered. Hydrogen probably dissociates heterolytically on adsorption, viz.

$$H_2 + M^{2+} + O^{2-} \rightarrow HM^+ + OH^-$$
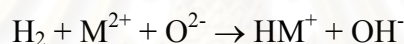
The hydroxyl ion will decompose on heating to form water and anion vacancies, and an equal number of cations will be reduced to atoms.

Carbon monoxide usually chemisorbed first on the cation, whence it reacts with an oxide ion:

$$(CO) \bullet\bullet\bullet M^+ + O^{2-} \rightarrow M + CO_2.$$
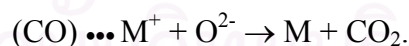
Here is the first stage of a process that can lead ultimately to the complete reduction of the oxide to metal. These steps are also similar to those involved in the catalyzed oxidation of these molecules.

The chemisorption of oxygen on p-type oxides occurs by a mechanism involving the oxidation of Ni^{2+} ions at the surface to Ni^{3+}:

$$2Ni^{2+} + O_2 \rightarrow 2(O^- \bullet\bullet\bullet Ni^{3+}).$$
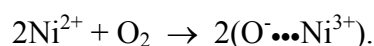
High coverages by the O⁻ ion can result, and it is easy to see that this is the first step in the incorporation of excess oxygen, referred to above. When the n-type oxides (exemplified by zinc oxide) are exactly stoichiometric, they cannot chemisorb oxygen: when however they are oxygen-deficient, they can chemisorb just as much as is needed to restore their stoichiometry by refilling the anion vacancies and reoxidizing the zinc atoms.

3.6 Adsorption on insulator oxides

Since the cations of insulator oxides can be neither oxidized nor reduced, they cannot chemisorb oxygen to any significant extent; they cannot chemisorb hydrogen or carbon monoxide for the same reason. They can, and do, react with water and other polar molecules as:

$$M^{x+} + O^{2-} \xrightarrow{\ H2O\ } (HO^- \bullet\bullet\bullet M^{x+}) + OH^-$$

$$M^{x+} + O^{2-} \xrightarrow{\ CH3OH\ } (CH_3O^- \bullet\bullet\bullet M^{x+}) + OH^-$$
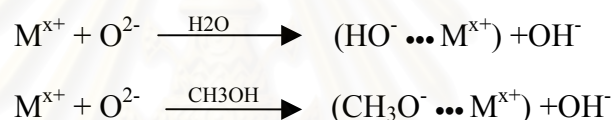
Indeed under normal circumstances the surface of oxides such as alumina and silica are covered by a layer of chemisorbed water: the surface is then said to be fully hydroxylated, and indeed these hydroxyl groups are very firmly bound. Their complete removal by heating is almost impossible. When the oxides are suspended in water the M-OH groups can dissociate either as acids or as bases, depending on the electronegativity of the cation, e.g.

$$Mg - OH \rightarrow Mg^{2+} + OH^-$$

$$Si - OH \rightarrow SiO^- + H^+$$
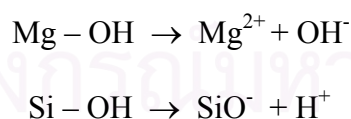
The variation of valence electron quantity causes the oxidation number change. These phenomenon leads to the electrical conductivity and acidity change (consider in case of Lewis acid).

CHAPTER IV

EXPERIMENTAL

The experimental systems and procedures used in this work are divided into three parts:

1. The preparation of catalysts.
2. The characterization of catalysts.
3. The catalytic activity measurements.

The details of the experiments are described as the following.

The scope of this study.

The reaction conditions are chosen as follows:

Catalysts	:	Cr-Mg-O/Al_2O_3, Mn-Mg-O/Al_2O_3,
		Mo-Mg-O/Al_2O_3, W-Mg-O/Al_2O_3,
		Fe-Mg-O/Al_2O_3, Zn-Mg-O/Al_2O_3
Reactant	:	$C_8H_4O_3$
Flow rate of reactant	:	100 ml/min
Reaction temperature	:	200-500°C
Space velocity	:	60 000 ml g^{-1} h^{-1}

4.1 Preparation of catalysts

4.1.1 Chemicals

The details of chemicals used in this experiment are shown in table 4.1.

Table 4.1 The chemicals used in this experiment.

Chemical	Grade	Supplier
Ammonium molybdate $((NH_4)_6Mo_7O_{24} \cdot 4H_2O)$	Analytical	Univar, Australia
Ammonium paratungstate $(H_{40}N_{10}O_{41}W_{12} \cdot 7H_2O)$	Analytical	Univar, Australia
Chromium nitrate nonahydrate $(CrN_3O_9 \cdot 9H_2O)$	Analytical	Fluka, Switzerland
Ferric nitrate nonahydrate $(FeN_3O_9 \cdot 9H_2O)$	Analytical	Fluka, Switzerland
Magnesium nitrate $(Mg(NO_3)_2)$	Analytical	Fluka, Switzerland
Manganese nitrate tetrahydrate $(Mn(NO_3)_2 \cdot 4H_2O)$	Analytical	Riedel-deHaen, Germany
Zinc nitrate hexahydrate $(ZnN_2O_6 \cdot 6H_2O)$	Analytical	Fluka, Switzerland
Alumina (Al_2O_3) JRC ALO2 (γ-phase)	Japan reference catalyst	Department of Material Science, Shimane University Catalysts and Chemicals Ind. Co., Ltd.

4.1.2 Preparation of catalyst

To study the effect of sequence of transition metal and magnesium loading, then three types of Cr-Mg-O/TiO$_2$ catalyst (8%wtCr, 4%wtMg) were prepared. In the first type of preparation, an appropriate amount of Al$_2$O$_3$ powder was added to an aqueous solution of chromium (III) nitrate nonahydrate (CrN$_3$O$_9$·9H$_2$O) at 70°C. The suspension was evaporated at 80°C, and then dried in the oven at 110°C in air over night. The resulting solid was calcined in air at 550°C for 6 hours. Magnesium was introduced into the calcined solid by impregnation from a magnesium nitrate (Mg(NO$_3$)$_2$) solution, evaporated at 80°C and dried at 110°C in air overnight. After drying the catalyst was calcined in air at 550°C for 6 hours. This catalyst was denoted as 8Cr4MgAl catalyst.

In the second type of sample, magnesium was firstly introduced in the way given above to the pure alumina support and then chromium was deposited on the Mg-doped Al$_2$O$_3$ support by the incipient wetness impregnation method. The catalyst was dried at 110°C in air overnight and calcined in air for 6 hours at 550°C. This catalyst was denoted as 4Mg8CrAl catalyst.

The third one was prepared by co-impregnation of chromium and magnesium. An appropriate Al$_2$O$_3$ was added to an aqueous solution containing both (CrN$_3$O$_9$·9H$_2$O) and Mg(NO$_3$)$_2$. The conditions of drying and calcination liked previous samples. This catalyst was denoted as co-8Cr4MgAl catalyst.

Three types of Mo-Mg-O/Al$_2$O$_3$, W-Mg-O/Al$_2$O$_3$, Mn-Mg-O/Al$_2$O$_3$ catalysts were prepared using similar method to the three types of Cr-Mg-O/Al$_2$O$_3$ catalysts. The symbols of the three types of Cr-Mg-O/Al$_2$O$_3$ catalysts liked the three types of Mo-Mg-O/Al$_2$O$_3$, W-Mg-O/Al$_2$O$_3$, Mn-Mg-O/Al$_2$O$_3$, Fe-Mg-O/Al$_2$O$_3$ and Zn-Mg-O/Al$_2$O$_3$ catalysts too i.e. 8Cr4MgAl, 4Mg8CrAl, co-8Cr4MgAl.

4.2 The characterization of catalyst

4.2.1 Determination of composition content of catalyst

The actual composition contents of all the catalysts were determined by atomic absorption spectroscopy (AAS) at the Department of Science Service, Ministry of Science Technology and Environment. The calculation of the sample preparation is shown in Appendix A.

4.2.2 BET Surface area measurement

4.2.2.1 Apparatus

The apparatus consisted of two gas feed lines for helium and nitrogen. The flow rate of gas was adjusted by means of a fine-metering valve. The sample cell was made from pyrex glass. The operation conditions of the gas chromatograph (GOW-MAC) is shown in Table 4.2

Table 4.2 Operation conditions of gas chromatograph (GOW-MAC)

Model	GOW-MAC
Detector	TCD
Helium flow rate	30 ml/min
Detector temperature	80°C
Detector current	80 mA

4.2.2.2 Procedure

The mixture of helium and nitrogen gas flowed through the system at the nitrogen gauge pressure of 0.3 atm. The sample was placed in the sample cell, which was then heated up to 150°C and held at this temperature for 2 h. The sample was cooled down to room temperature and ready to measure the surface area. There were three steps to measure the surface area.

(1) Adsorption step

The sample cell was dipped into a liquid nitrogen bath. Nitrogen was adsorbed on the surface of the sample until equilibrium was reached.

(2) Desorption step

The nitrogen-adsorbed sample was dipped into a water bath at room temperature. The adsorbed nitrogen was desorbed from the surface of the sample. This step was completed when the recorder line return back to the base line.

(3) Calibration step

1 ml of nitrogen gas at atmospheric pressure was injected at the calibration port and the area was measured. The area was used as the calibration peak.

(4) The BET surface area is calculated using procedures described in Appendix C.

4.2.3 X-ray diffraction (XRD)

The phase structures of the samples were determined by X-ray diffraction, Siemens D 5000 X-ray diffractometer using CuKα radiation with Ni filter in the 2θ range of 10-80°. The sample was placed into XRD plate before placing on the measured position of XRD diffractometer.

4.2.4 Pyridine Adsorption

The acid sites of the samples were determined by the pyridine adsorption. The apparatus consisted of the tube connected to the gas chromatograph (GC9A). The condition of the gas chromatograph is shown in Table 4.3.

Table 4.3 Operation conditions of gas chromatograph (GC9A)

Model	GC9A
Detector	FID
Nitrogen flow rate	30 ml/min
Column temperature	150°C
Detector temperature	180°C
Injector temperature	180°C

0.02 g of sample was placed in the tube. 0.01 µl of pyridine was injected to the gas chromatograph and the area was measure. The pyridine was injected until the sample was saturated. The acid site of the sample was calculated from the total area of the pyridine adsorbent.

4.2.5 Maleic anhydride Adsorption

The basic sites of the samples were determined by the maleic anhydride adsorption. The apparatus consisted of the tube connected to the gas chromatograph (GC9A). The condition of the gas chromatograph is shown in Table 4.4.

Table 4.4 Operation conditions of gas chromatograph (GC9A)

Model	GC9A
Detector	FID
Nitrogen flow rate	30 ml/min
Column temperature	280°C
Detector temperature	300°C
Injector temperature	300°C

0.03 g of sample was placed in the tube. 0.03 µl of maleic anhydride aqueous solution of a known concentration (10.4 g/100 ml) was injected to the gas chromatograph and the area was measure. The maleic anhydride was injected until

the sample was saturate. The basic site of the sample was calculated from the total area of the maleic anhydride adsorption.

4.3 The catalytic activity measurements

4.3.1 Equipment

The phthalic anhydride combustion system, as shown in Figure 4.1, consists of a reactor, a saturator, an automatic temperature controller, an electrical furnace and a gas controlling system.

The reactor is made from a stainless steel tube (O.D. 3/8"). Sampling points are provided above and below the catalyst bed. Catalyst is placed between two quartz wool layers.

An automatic temperature controller consists of a magnetic contractor model Telex 87114. Reactor temperature was measured at the bottom of the catalyst bed in the reactor. The temperature control set point is adjustable within the range of 0-800°C at the maximum voltage output of 220 volt.

The electrical furnace supplies heat to the reactor for phthalic anhydride combustion. The reactor can be operated from room temperature up to 800°C at the maximum voltage of 220 volt.

The gas supplying system consists of cylinders of air zero, each equipped with pressure regulators (0-120 psig), on-off valves and fine-meter valves used for adjusting the flow rate.

The composition in the feed and product stream was analyzed by flame ionization detector gas Chromatograph Shimadzu GC9A.
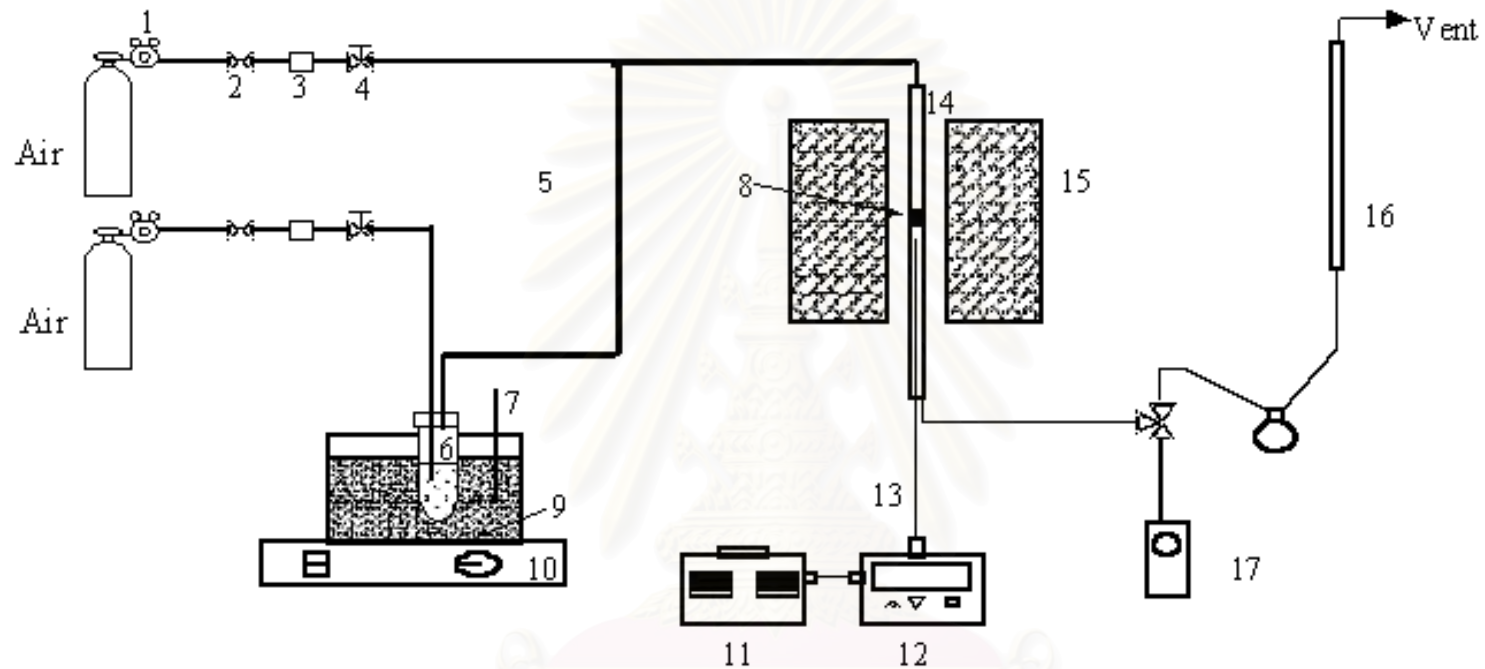
1. Pressure Regulator   2. On-Off Valve   3. Gas Filter   4. Metering Valve

5. Heating Line   6. Saturator   7. Thermometer   8. Catalyst Bed

9. Sand   10. Stirring Controller   11. Variable Voltage Transformer   12. Temperature Controller

13. Thermocouple   14. Reactor   15. Furnace   16. Flow Meter

17. Sampling point

Figure 4.1 Flow diagram of phthalic anhydride combustion system

A Shimadzu GC8A gas chromatograph equipped with a thermal conductivity detector was used to analyze permanent gases and water. Two columns, a 5A molecular sieve to separate oxygen and CO and a Porapak-Q column to separate CO_2 and water were operated in parallel. The operating conditions of the GC are listed in the Table 4.5.

Table 4.5 Operating conditions for gas chromatographs

Gas chromatograph	GC8A	GC9A
Detector	TCD	FID
Column	MS-5A, Porapak-Q	Chromosorb WAW
Carrier gas	He (99.999%)	N_2 (99.999%)
Carrier gas flow	25 ml/min	30 ml/min
Column temperature		
- Initial	100 °C	210°C
- Final	100 °C	210°C
Detector temperature	130 °C	250°C
Injector temperature	130 °C	250°C
Analyzed gas	CO, CO_2, H_2O	phthalic anhydride

4.3.2 Oxidation procedure

The oxidation procedures are described in the detail below.

1. 0.1 gram of catalyst was packed in the middle of the stainless steel microreactor located in an electrical furnace.
2. The total flow rate was 100 ml/min. The concentration of phthalic anhydride in air was adjusted to the required values.
3. The reaction temperature was between 200-500°C. The effluent gas was analyzed by using the FID and TCD gas chromatograph. The chromatograph data were changed into mole of maleic anhydride, phthalic anhydride and CO_2 by calibration curves in Appendix D.

The operating conditions selected have been checked to confirm that there is no external and internal mass transfer resistance. The calculation is shown in Appendix B.

CHAPTER V

RESULTS AND DISCUSSION

The results and discussion in this chapter are divided into two major parts including the catalyst characterization and the catalytic combustion reaction of phthalic anhydride.

5.1 Catalyst characterization

5.1.1 Determination of composition content and BET surface area of catalyst

The results of metal composition and BET surface area of all catalysts, which are analyzed by Atomic Absorption Spectroscopy (AAS) and BET surface area are summarized in Tables 5.1.

Table 5.1 The composition of different order magnesium loading sequence catalyst and BET surface area

Catalyst	Wt% Metal	wt% Mg	BET surface area (m^2/g)
co-8Cr-4Mg-O/Al$_2$O$_3$	7.8	3.9	100.91
8Cr-4Mg-O/Al$_2$O$_3$	7.6	3.6	92.90
4Mg-8Cr-O/Al$_2$O$_3$	7.6	3.9	88.63
co-8Mn-4Mg-O/Al$_2$O$_3$	7.9	3.7	114.55
8Mn-4Mg-O/Al$_2$O$_3$	7.5	3.6	94.91
4Mg-8Mn-O/Al$_2$O$_3$	7.7	3.8	124.56
co-8Mo-4Mg-O/Al$_2$O$_3$	7.9	3.8	90.29
8Mo-4Mg-O/Al$_2$O$_3$	7.8	3.6	110.52
4Mg-8Mo-O/Al$_2$O$_3$	7.6	3.7	94.63
co-8W-4Mg-O/Al$_2$O$_3$	8.1	3.9	121.86
8W-4Mg-O/Al$_2$O$_3$	7.9	3.7	99.19
4Mg-8W-O/Al$_2$O$_3$	7.6	3.5	96.34
co-8Fe-4Mg-O/Al$_2$O$_3$	7.9	3.8	89.69
8Fe-4Mg-O/Al$_2$O$_3$	7.5	3.9	85.14
4Mg-8Fe-O/Al$_2$O$_3$	7.6	3.8	95.12
co-8Zn-4Mg-O/Al$_2$O$_3$	7.8	3.7	106.96
8Zn-4Mg-O/Al$_2$O$_3$	7.5	3.5	102.63
4Mg-8Zn-O/Al$_2$O$_3$	7.3	3.6	99.57
Al$_2$O$_3$	-	-	130.38

สถาบันวิทยบริการ
จุฬาลงกรณ์มหาวิทยาลัย

The above data in Table 5.1 indicate that the transition metal oxide and magnesium contents in sample are close to calculated value. The correlation between the transition metal oxide and magnesium amounts and the surface area could not be defined. It can be seen that the surface area of the catalysts, prepared in different order metal loading, are quite the same. Therefore, the sequence of metal and magnesium loading seems to have no effect on the surface area.

5.1.2 X-ray Diffraction (XRD)

The crystal structure of the catalysts was identified by X-ray diffraction technique. The first three strongest XRD peaks of transition metal oxides from the reference [The JCPDS (1980)] using CuKα radiation are listed in Table 5.2.

Table 5.2 The reference of XRD Pattern for transition metal oxide catalysts

Oxides	Position (2θ)	Oxides	Position (2θ)
CrO_3	14.2°, 25.8°, 26.2°	WO_2	25.8°, 36.8°, 37°
Cr_2O_3	33.6°, 36.2°, 54.6°	Fe_2O_3	29.8°, 32.8°, 67.5°
CrO	34.6°, 44.4°, 48°	FeO	61°, 61.4°, 73°
MnO	20.2°, 21.6°, 36.4°	ZnO	33.6°, 58.4°, 62.6°
MnO_2	21.8°, 35.8°, 55°	ZnO_2	31.8°, 37°, 63°
Mn_3O_4	18.2°, 35.4°, 62°	CuO	35.4°, 35.6°, 38.8°
Mn_2O_3	32.2°, 35.6°, 53°	Cu_2O	37°, 40.4°, 42.4°
MoO_3	9.6°, 25.8°, 29.4°	Ni_2O_3	32°, 44.8°, 51.6°
MoO_2	26°, 36.8°, 53.4°	NiO	37.2°, 43.2°, 62.6°
WO_3	24°, 33°, 55°	MgO	37°, 43°, 62.8°

If the catalysts studied contained a transition metal oxide form, some of the peaks shown in Table 5.2 should appear in the XRD spectra. But from the Figures 5.1-5.6, all of the catalysts investigated did not show any peak of these transition metal oxides. All of the catalysts showed the XRD patterns in the same position as Al_2O_3 support that showed 4 peaks at $37°$, $45°$, $46°$, and $65.5°$. The peaks of these transition metal oxides were not detected possibly because the XRD patterns of these transition metal oxides were hidden by the XRD pattern of Al_2O_3 support, the oxides did not form a crystal with significant size or it did not form a crystal.

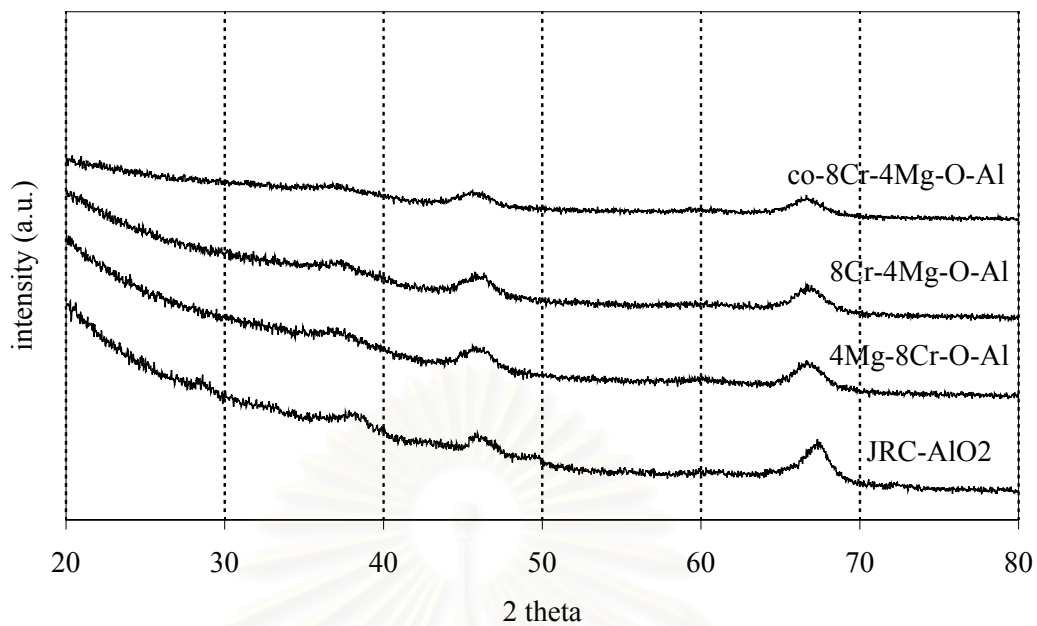**Figure 5.1** The XRD pattern of JRC-AlO2, 4Mg-8Cr-O-Al, 8Cr-4Mg-O-Al and co-8Cr-4Mg-O-Al catalysts

Figure 5.2 The XRD pattern of JRC-AlO2, 4Mg-8Mn-O-Al, 8Mn-4Mg-O-Al and co-8Mn-4Mg-O-Al catalysts

Figure 5.3 The XRD pattern of JRC-AlO2, 4Mg-8Mo-O-Al, 8Mo-4Mg-O-Al and co-8Mo-4Mg-O-Al catalysts
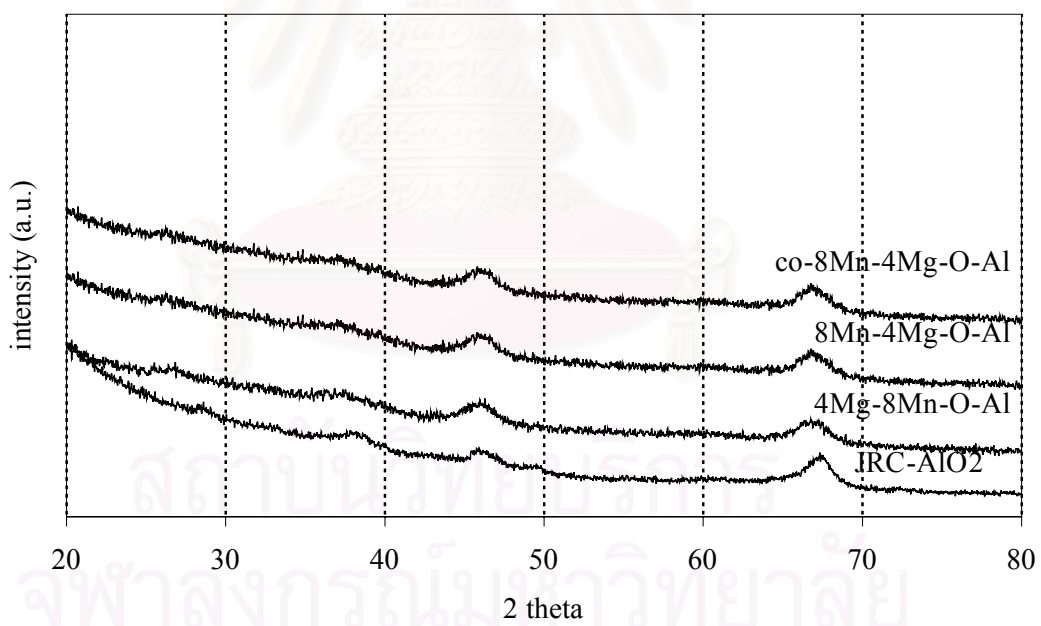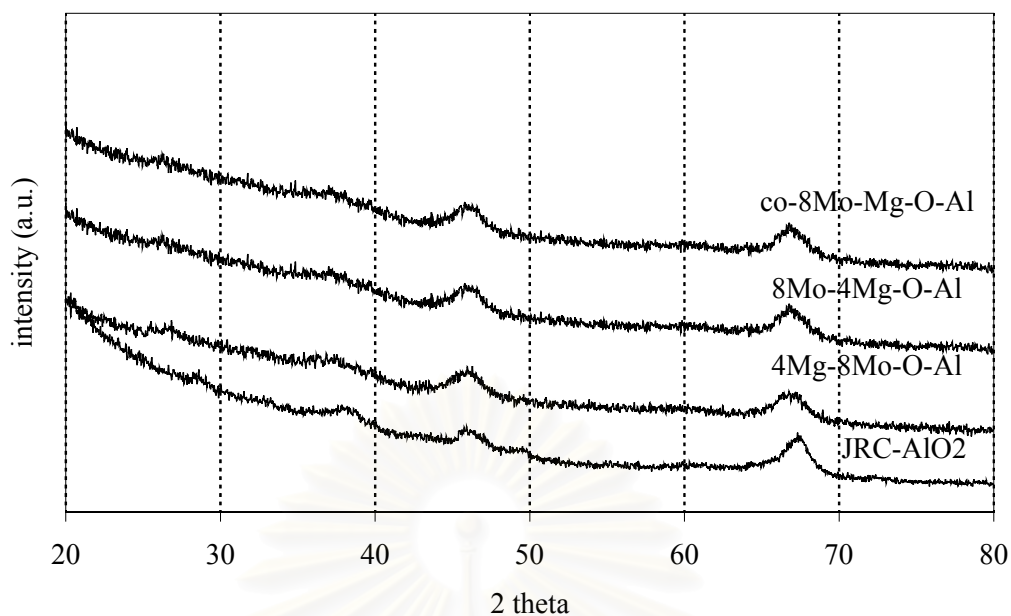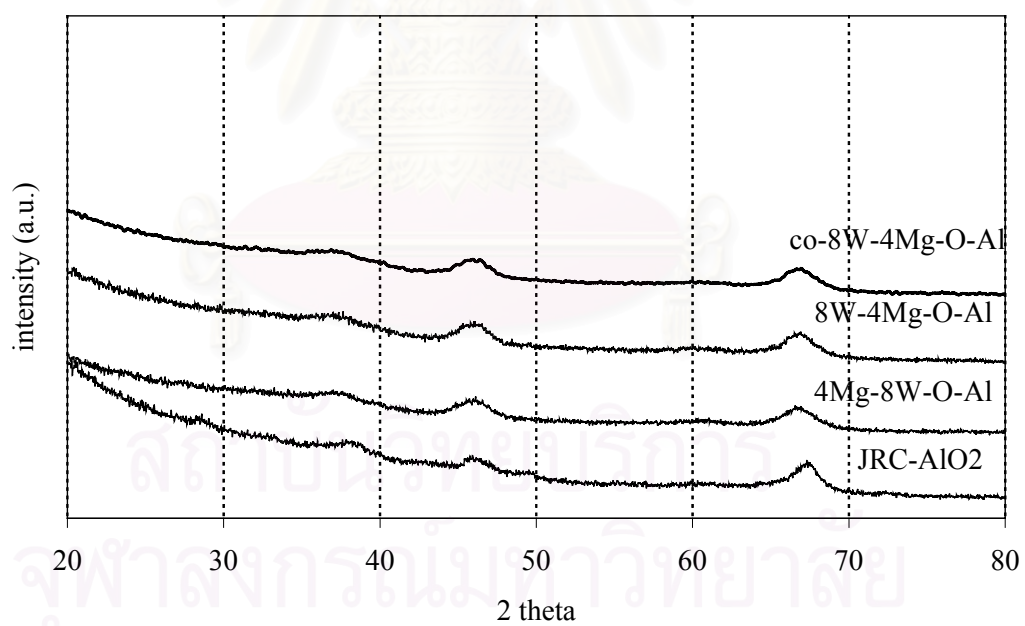

Figure 5.4 The XRD pattern of JRC-AlO2, 4Mg-8W-O-Al, 8W-4Mg-O-Al and co-8W-4Mg-O-Al catalysts
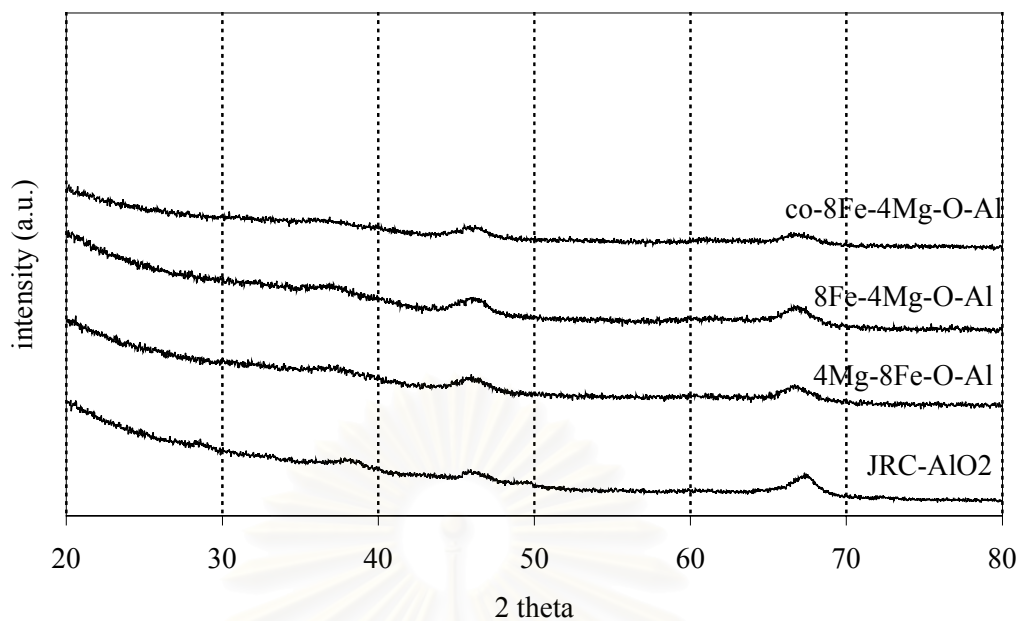
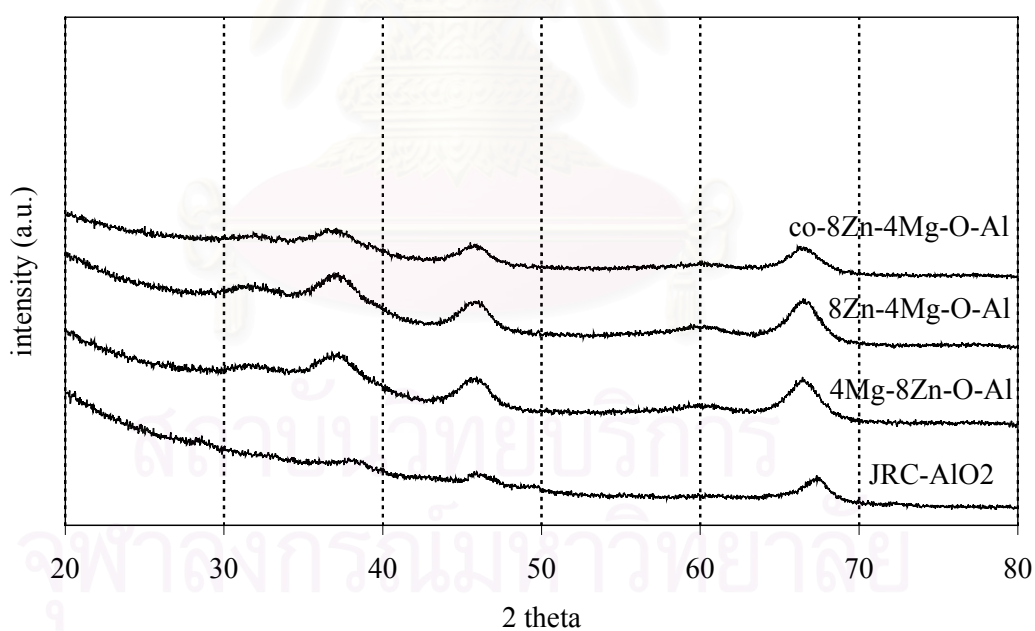**Figure 5.5** The XRD pattern of JRC-AlO2, 4Mg-8Fe-O-Al, 8Fe-4Mg-O-Al and co-8Fe-4Mg-O-Al catalysts

Figure 5.6 The XRD pattern of JRC-AlO2, 4Mg-8Zn-O-Al, 8Zn-4Mg-O-Al and co-8Zn-4Mg-O-Al catalysts

5.2 Catalytic reaction

Phthalic anhydride comprises of an anhydride functional group and a benzene ring. It is a product in the oxidation of o-xylene. In this work, the effects of transition metal and magnesium loading sequence on the combustion of phthalic anhydride were received much attention. This reaction was studied in an excess oxygen atmosphere. The combustion reaction was as followed:

$$C_8H_4O_3 + 7.5\ O_2 \longrightarrow 8\ CO_2 + 2\ H_2O$$
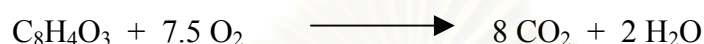
There were only a few studies about the combustion reaction of phthalic anhydride. The Co-Mg-O/Al$_2$O$_3$ and V-Mg-O/TiO$_2$ were used as catalysts for this reaction. The result of using Co-Mg-O/Al$_2$O$_3$ and V-Mg-O/TiO$_2$ catalysts showed that magnesium oxide could promote the adsorption of phthalic anhydride leading to better combustion of phthalic anhydride. In the concurrent research, it is toward that some supported acidic transition metal oxides (Cr, Mn, Mo and W) and some amphoteric transition metal oxides (Fe and Zn) promoted with MgO show higher phthalic anhydride combustion activity than the base oxide. The present work is a co-current research work which investigates a parameter affecting the catalytic activity of the catalysts. The parameter investigated here is the sequence of metal loading. The important of this parameter is mention previously in Chapter I. The chosen catalysts were the oxide of Cr, Mn, Mo, W, Fe and Zn. These catalysts were divided into 2 groups as follow :

    Acidic transition metal oxide catalysts   :   Cr, Mn, Mo, and W

    Amphoteric transition metal oxide catalysts :   Fe, and Zn

5.2.1 Acidic transition metal oxide catalysts

5.2.1.1 Chromium oxide catalysts

Figure 5.7 shows the phthalic anhydride conversion over chromium oxide catalysts. The amount of chromium was fixed at 8% by weight and magnesium was fixed at 4% by weight. It was found that $4Mg-8Cr-O/Al_2O_3$ showed the best conversion, which increased from 7.5 to 79% in the range of temperature 200 to 300° C and raised to 100% conversion at 350°C. While $8Cr-4Mg-O/Al_2O_3$ exhibited the phthalic anhydride conversion as about 9.4 to 94% in the range of temperature 200 to 350°C and raised to 100% conversion at 400°C and $co-8Cr-4Mg-O/Al_2O_3$ exhibited the phthalic anhydride conversion as about 9.7 to 93% in the range of temperature 200 to 350°C and raised to 100% conversion at 400°C. The catalytic activity of these catalysts was in the order of $4Mg-8Cr-O/Al_2O_3 > 8Cr-4Mg-O/Al_2O_3 > co-8Cr-4Mg-O/Al_2O_3$.

The pyridine and maleic anhydride adsorption of the chromium oxide catalysts related to Al_2O_3 is shown in Table 5.3

Table 5.3 The relative amounts of pyridine and maleic anhydride adsorption of the chromium oxide

Catalyst	Pyridine		Maleic anhydride	
	Relative	nmol/m^2	Relative	nmol/m^2
Al_2O_3	1.000	0.0172	1.00	6.30
$co-8Cr-4Mg-O/Al_2O_3$	0.912	0.0157	1.32	8.31
$8Cr-4Mg-O/Al_2O_3$	0.917	0.0158	1.28	8.06
$4Mg-8Cr-O/Al_2O_3$	0.920	0.0158	1.25	7.87

The results showed that the acidity of the catalysts were similar but the basicity of the catalysts were not similar. The basicity was in the order of $4Mg-8Cr-O/Al_2O_3 < 8Cr-4Mg-O/Al_2O_3 < co-8Cr-4Mg-O/Al_2O_3$.
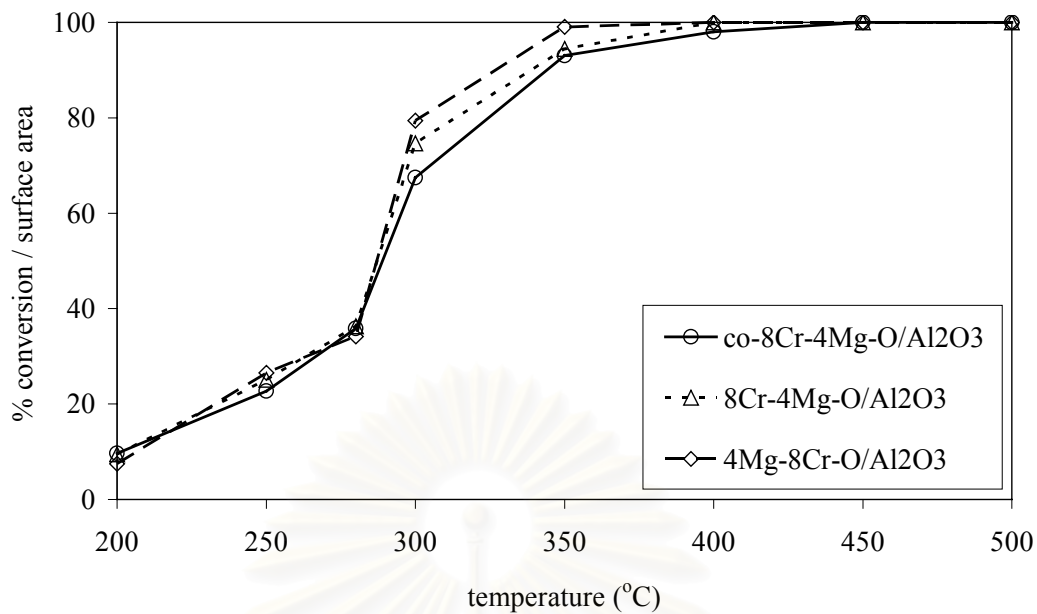
Figure 5.7 Catalytic activity of 8Cr-4Mg-O/Al$_2$O$_3$ catalysts system base on surface area of catalyst for the combustion of phthalic anhydride

5.2.1.2 Manganese oxide catalysts

Figure 5.8 shows the catalytic activity of $Mn-Mg-O/Al_2O_3$ catalyst for phthalic anhydride combustion. The amount of manganese was fixed at 8% by weight and magnesium was fixed at 4% by weight. It was found that $4Mg-8Mn-O/Al_2O_3$ showed the best conversion, which increased from 2.7 to 87% in the range of temperature 200 to 400°C and raised to 100% conversion at 450°C. While $co-8Mn-4Mg-O/Al_2O_3$ exhibited the phthalic anhydride conversion as about 2.3 to 75% in the range of temperature 200 to 350°C and raised to 100% conversion at 400°C and $8Mn-4Mg-O/Al_2O_3$ exhibited the phthalic anhydride conversion as about 1.7 to 95% in the range of temperature 200 to 350°C and raised to 100% conversion at 400°C. The catalytic activity of these catalysts was in the order of $4Mg-8Mn-O/Al_2O_3 > co-8Mn-4Mg-O/Al_2O_3 > 8Mn-4Mg-O/Al_2O_3$.

The pyridine and maleic anhydride adsorption of the manganese oxides catalysts related to Al_2O_3 is shown in Table 5.4

Table 5.4 The relative amounts of pyridine and maleic anhydride adsorption of the manganese oxide

Catalyst	Pyridine		Maleic anhydride	
	Relative	$nmol/m^2$	Relative	$nmol/m^2$
Al_2O_3	1.000	0.0172	1.00	6.30
$co-8Mn-4Mg-O/Al_2O_3$	1.592	0.0274	1.05	6.61
$8Mn-4Mg-O/Al_2O_3$	1.568	0.0270	1.08	6.80
$4Mg-8Mn-O/Al_2O_3$	1.604	0.0276	1.03	6.48

The results showed that the acidity of the catalysts were similar but the basicity of the catalysts were not similar. The basicity was in the order of $4Mg-8Mn-O/Al_2O_3 < co-8Mn-4Mg-O/Al_2O_3 < 8Mn-4Mg-O/Al_2O_3$.
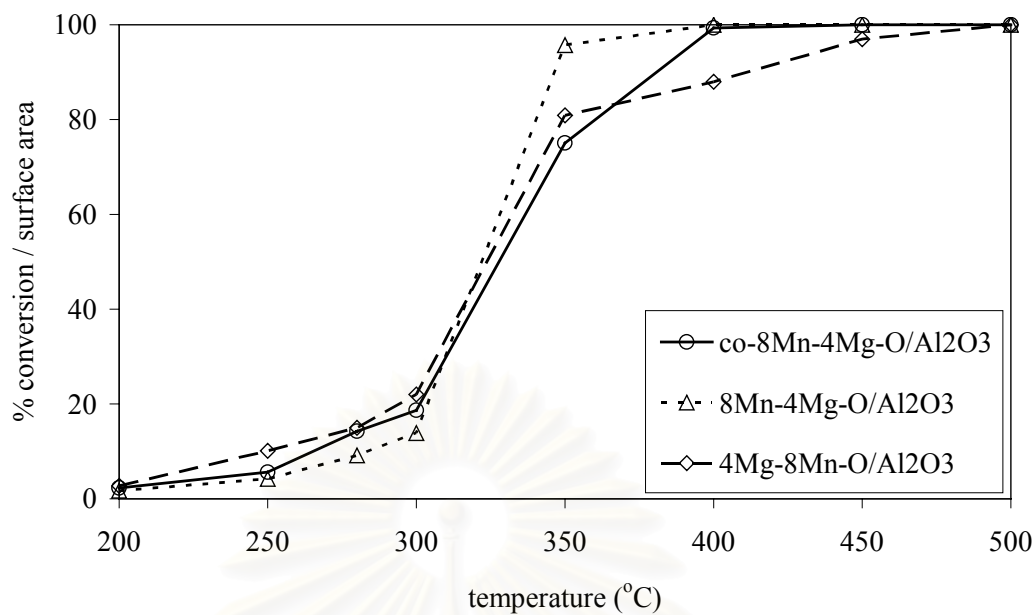
Figure 5.8 Catalytic activity of 8Mn-4Mg-O/Al$_2$O$_3$ catalysts base on surface area of catalyst for the combustion of phthalic anhydride

5.2.1.3 Molybdenum oxide catalysts

Figure 5.9 shows the catalytic activity of Mo-Mg-O/Al$_2$O$_3$ catalyst for phthalic anhydride combustion. The amount of manganese was fixed at 8% by weight and magnesium was fixed at 4% by weight. It was found that co-8Mo-4Mg-O/Al$_2$O$_3$ showed the best conversion, which increased from 1.4 to 47% in the range of temperature 200 to 300°C and raised to 100% conversion at 350°C. While 8Mo-4Mg-O/Al$_2$O$_3$ exhibited the phthalic anhydride conversion as about 1.8 to 94% in the range of temperature 200 to 400°C and raised to 100% conversion at 450°C and 4Mg-8Mo-O/Al$_2$O$_3$ exhibited the phthalic anhydride conversion as about 2.2 to 22% in the range of temperature 200 to 300°C and raised to 100% conversion at 350°C. The catalytic activity of these catalysts was in the order of co-8Mo-4Mg-O/Al$_2$O$_3$ > 8Mo-4Mg-O/Al$_2$O$_3$ > 4Mg-8Mo-O/Al$_2$O$_3$.

The pyridine and maleic anhydride adsorption of the molybdenum oxides catalysts related to Al$_2$O$_3$ is shown in Table 5.5

Table 5.5 The relative amounts of pyridine and maleic anhydride adsorption of the molybdenum oxide

Catalyst	Pyridine		Maleic anhydride	
	Relative	nmol/m^2	Relative	nmol/m^2
Al$_2$O$_3$	1.000	0.0172	1.00	6.30
co-8Mo-4Mg-O/Al$_2$O$_3$	1.664	0.0286	0.75	4.72
8Mo-4Mg-O/Al$_2$O$_3$	1.605	0.0276	0.78	4.91
4Mg-8Mo-O/Al$_2$O$_3$	1.577	0.0271	0.80	5.04

The results showed that the acidity of the catalysts were similar but the basicity of the catalysts were not similar. The basicity was in the order of co-8Mo-4Mg-O/Al$_2$O$_3$ < 8Mo-4Mg-O/Al$_2$O$_3$ < 4Mg-8Mo-O/Al$_2$O$_3$.
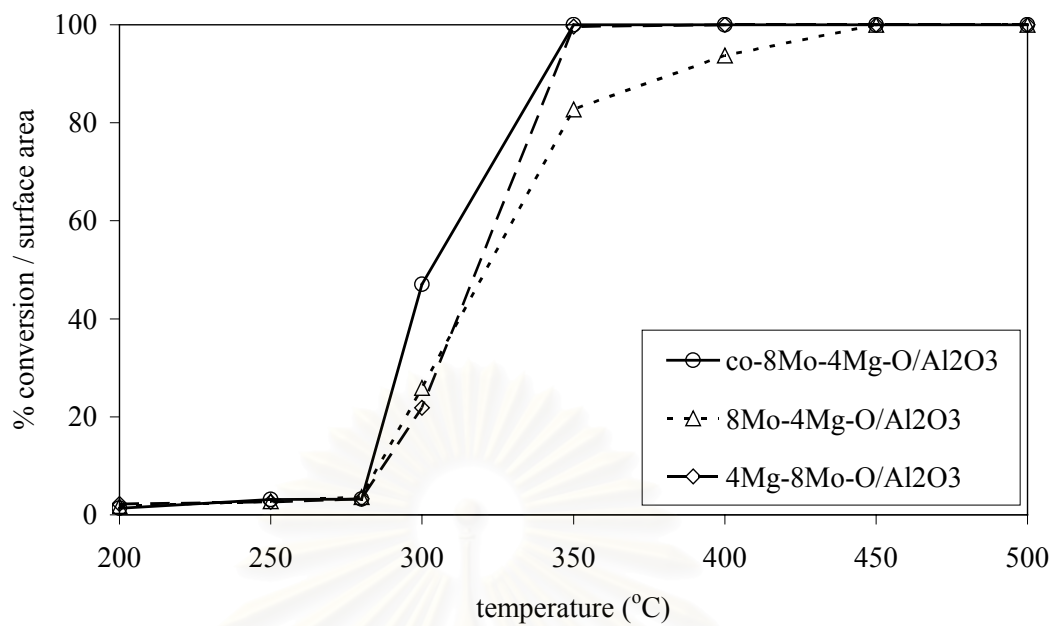
Figure 5.9 Catalytic activity of 8Mo-4Mg-O/Al$_2$O$_3$ catalysts base on surface area of catalyst for the combustion of phthalic anhydride

5.2.1.4 Tungsten oxide catalysts

Figure 5.10 shows the phthalic anhydride conversion over chromium oxide catalysts. The amount of chromium was fixed at 8% by weight and magnesium was fixed at 4% by weight. It was found that 4Mg-8W-O/Al$_2$O$_3$ showed the best conversion, which increased from 1.3 to 75% in the range of temperature 200 to 300° C and raised to 100% conversion at 350°C. While 8W-4Mg-O/Al$_2$O$_3$ exhibited the phthalic anhydride conversion as about 1.7 to 68% in the range of temperature 200 to 300°C and raised to 100% conversion at 350°C and co-8W-4Mg-O/Al$_2$O$_3$ exhibited the phthalic anhydride conversion as about 3 to 85% in the range of temperature 200 to 350°C and raised to 100% conversion at 400°C. The catalytic activity of these catalysts was in the order of 4Mg-8W-O/Al$_2$O$_3$ > 8W-4Mg-O/Al$_2$O$_3$ > co-8W-4Mg-O/Al$_2$O$_3$.

The pyridine and maleic anhydride adsorption of the tungsten oxides catalysts related to Al$_2$O$_3$ is shown in Table 5.6

Table 5.6 The relative amounts of pyridine and maleic anhydride adsorption of the tungsten oxide

Catalyst	Pyridine		Maleic anhydride	
	Relative	nmol/m^2	Relative	nmol/m^2
Al$_2$O$_3$	1.000	0.0172	1.00	6.30
co-8W-4Mg-O/Al$_2$O$_3$	1.568	0.0270	1.48	9.30
8W-4Mg-O/Al$_2$O$_3$	1.551	0.0267	1.51	9.50
4Mg-8W-O/Al$_2$O$_3$	1.506	0.0259	1.54	9.72

The results showed that the acidity of the catalysts were similar but the basicity of the catalysts were not similar. The basicity was in the order of 4Mg-8W-O/Al$_2$O$_3$ > 8W-4Mg-O/Al$_2$O$_3$ > co-8W-4Mg-O/Al$_2$O$_3$.
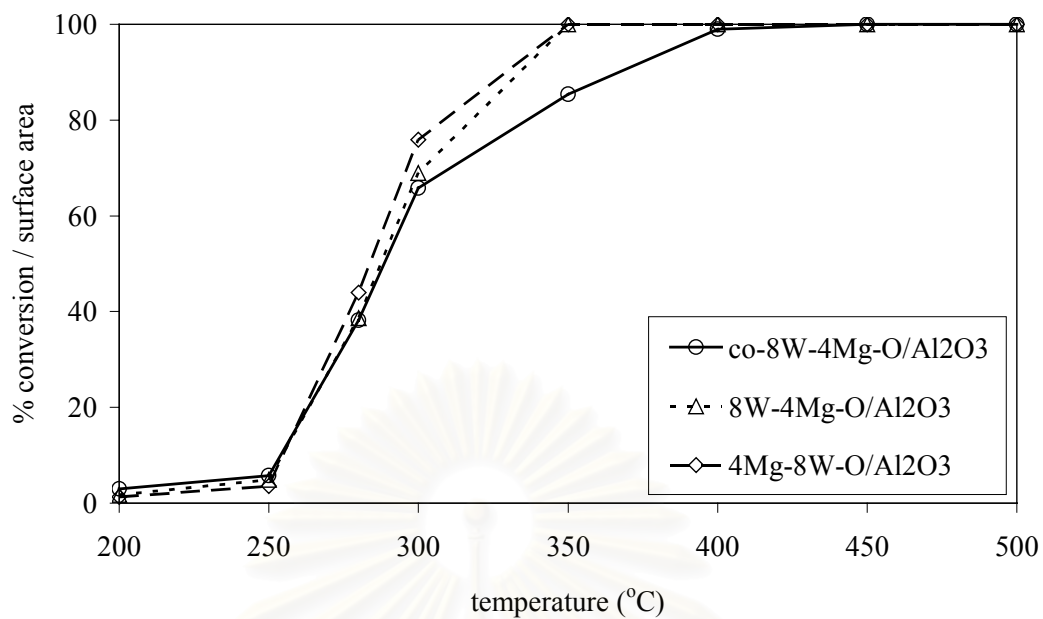
Figure 5.10 Catalytic activity of 8W-4Mg-O/Al$_2$O$_3$ catalysts base on surface area of catalyst for the combustion of phthalic anhydride

5.2.2 Amphoteric transition metal oxide catalysts

5.2.2.1 Iron oxide catalysts

Figure 5.11 shows the catalytic activity of Fe-Mg-O/Al$_2$O$_3$ catalyst for phthalic anhydride combustion. The amount of manganese was fixed at 8% by weight and magnesium was fixed at 4% by weight. It was found that 4Mg-8Fe-O/Al$_2$O$_3$ showed the best conversion, which increased from 0.6 to 91% in the range of temperature 200 to 400°C and raised to 100% conversion at 450°C. While co-8Fe-4Mg-O/Al$_2$O$_3$ exhibited the phthalic anhydride conversion as about 0 to 73% in the range of temperature 200 to 350°C and raised to 100% conversion at 400°C and 8Fe-4Mg-O/Al$_2$O$_3$ exhibited the phthalic anhydride conversion as about 0.5 to 76% in the range of temperature 200 to 350°C and raised to 100% conversion at 400°C. The catalytic activity of these catalysts was in the order of 4Mg-8Fe-O/Al$_2$O$_3$ > co-8Fe-4Mg-O/Al$_2$O$_3$ $\approx$ 8Fe-4Mg-O/Al$_2$O$_3$.

The pyridine and maleic anhydride adsorption of the ion oxides catalysts related to Al$_2$O$_3$ is shown in Table 5.7

Table 5.7 The relative amounts of pyridine and maleic anhydride adsorption of the ion oxide

Catalyst	Pyridine		Maleic anhydride	
	Relative	nmol/m^2	Relative	nmol/m^2
Al$_2$O$_3$	1.000	0.01720	1.00	6.30
co-8Fe-4Mg-O/Al$_2$O$_3$	0.550	0.00946	1.70	10.70
8Fe-4Mg-O/Al$_2$O$_3$	0.553	0.00951	1.69	10.64
4Mg-8Fe-O/Al$_2$O$_3$	0.602	0.01040	1.65	10.39

The results showed that the acidity of the catalysts were similar but the basicity of the catalysts were not similar. The basicity was in the order of 4Mg-8Fe-O/Al$_2$O$_3$ < 8Fe-4Mg-O/Al$_2$O$_3$ < co-8Fe-4Mg-O/Al$_2$O$_3$.
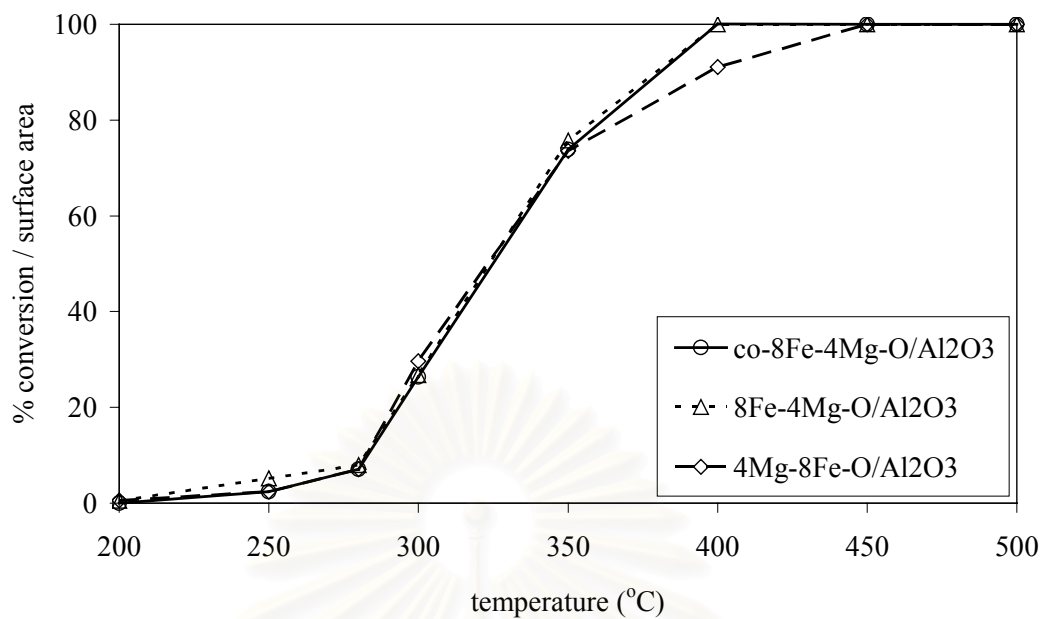
Figure 5.11 Catalytic activity of 8Fe-4Mg-O/Al$_2$O$_3$ catalysts base on surface area of catalyst for the combustion of phthalic anhydride

5.2.2.2 Zinc oxide catalysts

Figure 5.12 shows the phthalic anhydride conversion over zinc oxide catalysts. The amount of zinc was fixed at 8% by weight and magnesium was fixed at 4%. It was found that co-8Zn-4Mg-O/Al$_2$O$_3$ showed the best conversion, which increased from 1.2 to 90% in the range of temperature 200 to 350°C and raised to 100% conversion at 400°C. While 8Zn-4Mg-O/Al$_2$O$_3$ exhibited the phthalic anhydride conversion as about 0.4 to 82% in the range of temperature 200 to 350°C and raised to 100% conversion at 400°C and 4Mg-8Zn-O/Al$_2$O$_3$ exhibited the phthalic anhydride conversion as about 1.9 to 67% in the range of temperature 200 to 350°C and raised to 100% conversion at 400°C. The catalytic activity of these catalysts was in the order of co-8Zn-4Mg-O/ Al$_2$O$_3$ > 8Zn-4Mg-O/Al$_2$O$_3$ > 4Mg-8Zn-O/Al$_2$O$_3$.

The pyridine and maleic anhydride adsorption of the zinc oxides catalysts related to Al$_2$O$_3$ is shown in Table 5.8

Table 5.8 The relative amounts of pyridine and maleic anhydride adsorption of the zinc oxide

Catalyst	Pyridine		Maleic anhydride	
	Relative	nmol/m^2	Relative	nmol/m^2
Al$_2$O$_3$	1.000	0.0172	1.00	6.30
co-8Zn-4Mg-O/Al$_2$O$_3$	0.595	0.0102	1.43	9.00
8Zn-4Mg-O/Al$_2$O$_3$	0.580	0.0098	1.47	9.27
4Mg-8Zn-O/Al$_2$O$_3$	0.588	0.0101	1.51	9.50

The results showed that the acidity of the catalysts were similar but the basicity of the catalysts were not similar. The basicity was in the order of co-8Zn-4Mg-O/Al$_2$O$_3$ < 8Zn-4Mg-O/Al$_2$O$_3$ < 4Mg-8Zn-O/Al$_2$O$_3$ and the catalytic activity was in the order of co-8Zn-4Mg-O/Al$_2$O$_3$ > 8Zn-4Mg-O/Al$_2$O$_3$ > 4Mg-8Zn-O/Al$_2$O$_3$.
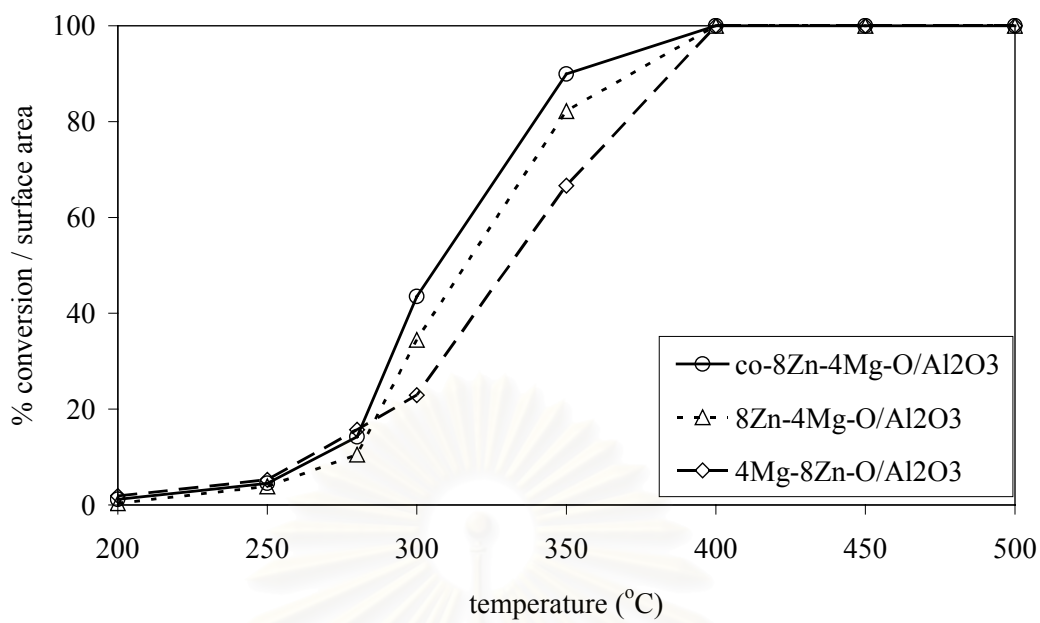
Figure 5.12 Catalytic activity of 8Zn-4Mg-O/Al$_2$O$_3$ catalysts base on surface area of catalyst for the combustion of phthalic anhydride

5.3 Activity and surface acidity/basicity

The surface acidity and basicity of the catalysts could be evaluated by the amount of pyridine and maleic anhydride adsorption, respectively. The amount of pyridine adsorbed represents the numbers of acid sites. The amount of maleic anhydride adsorbed represents the numbers of basic sites. The adsorption of maleic anhydride also indicated the ability of the catalyst to adsorb an acidic reactant, that was phthalic anhydride in this work. Thus, the large amount of maleic anhydride adsorption would have the large numbers of adsorption sites.

In this works, it is hypothesised that the acid site was the active site. The basic site (MgO) would help the adsorption of the acidic reactant, but in the same time, these basic promoter would neutralize the acid site (active site). Thus, the maximum activity of the phthalic anhydride combustion needed the optimum between the amount of metal and MgO. The maximum of the activity and wt% magnesium on the catalysts can be graphically showed in Figure 5.13. When the basicity increased, the activity increased and remains increased until reaching a point that had the maximum activity. In this region, the destruction of active site was compensated by the enhance adsorption of the reactant. After that, if more base was added to the catalysts, the activity would decrease, due to too many active sites were destroyed. Thus, the maximum activity point is the point that had the optimum between the metal oxide and magnesium oxide.
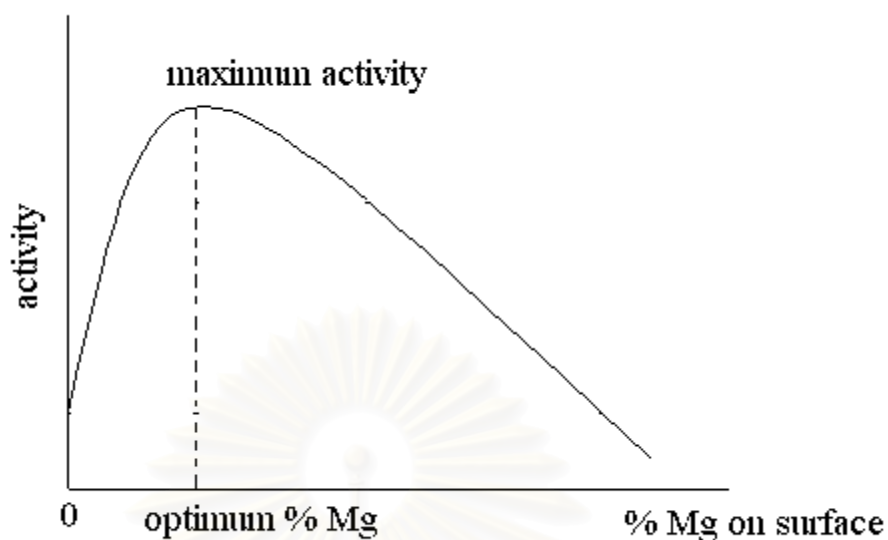
Figure 5.13 The optimum of % magnesium on surface and activity

In order to determine the position of the catalyst studied in this work on the graph, a comparison with catalysts with different Mg loading has to be carried out. The results of catalysts doped with 1 wt% and 10 wt% Mg were taken from the work of Nugoolchit (2002). Using the results from the work of Nugoolchit we can divide the catalyst investigated in this research into 2 groups as follows:

1. 4 wt% Mg is better than 1 wt% and 10 wt% Mg (Cr, Mo, W and Fe) (Figures 5.14 - 5.17)

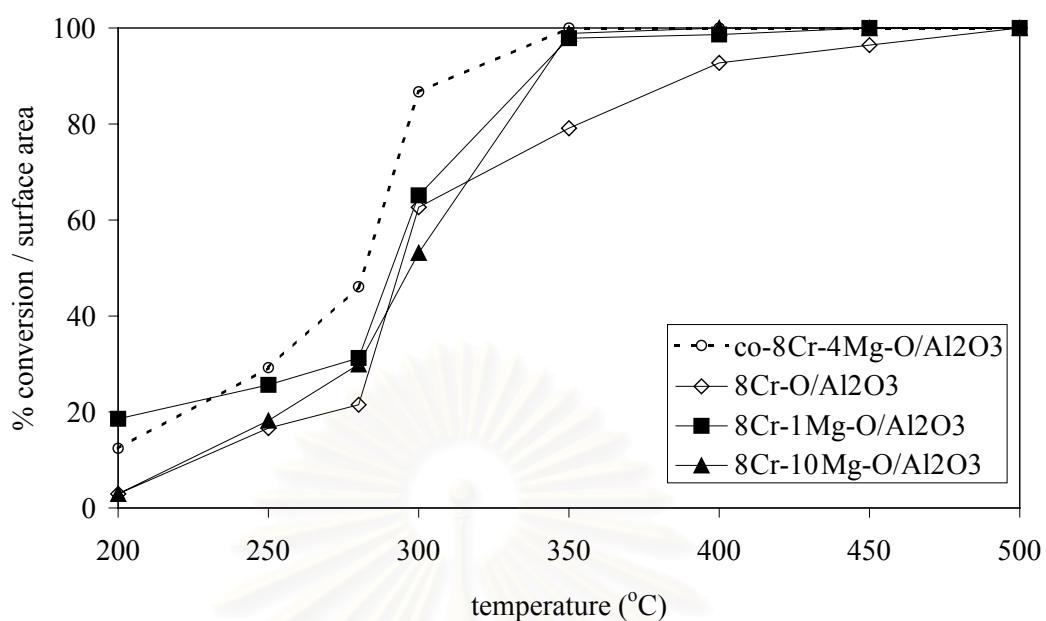2. 4 wt% Mg is worse than 1 wt% but better than 10 wt% Mg (Mn and Zn) (Figures 5.18 - 5.19)

Figure 5.14 The catalytic activity of chromium oxide catalysts base on surface area of catalyst for the combustion of phthalic anhydride

Figure 5.15 The catalytic activity of molybdenum oxide catalysts base on surface area of catalyst for the combustion of phthalic anhydride

Figure 5.16 The catalytic activity of tungsten oxide catalysts base on surface area of catalyst for the combustion of phthalic anhydride
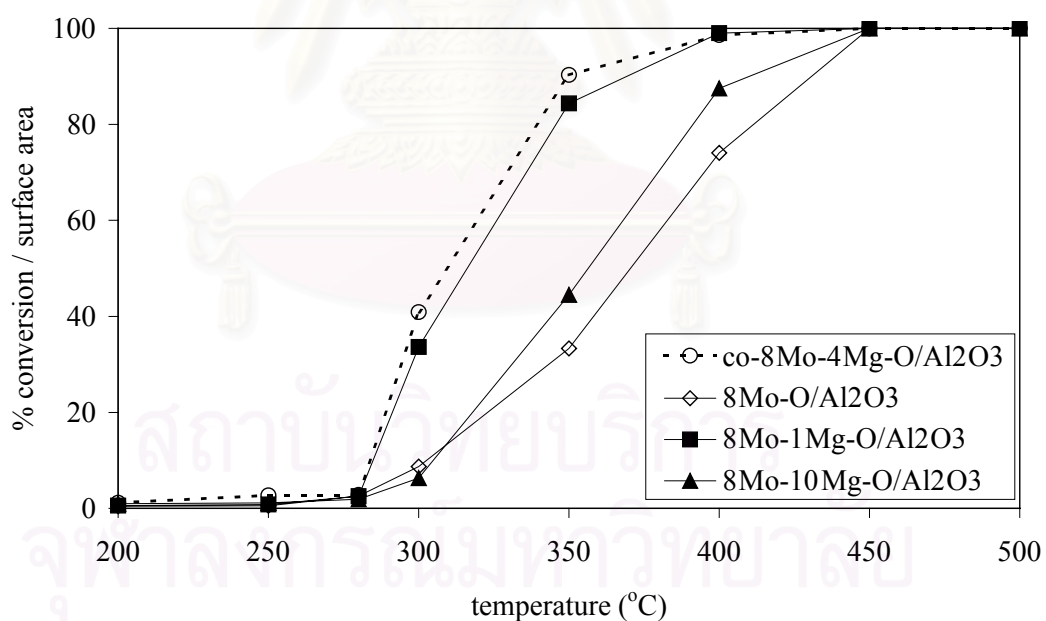

Figure 5.17 The catalytic activity of ion oxide catalysts base on surface area of catalyst for the combustion of phthalic anhydride

Figure 5.18 The catalytic activity of manganese oxide catalysts base on surface area of catalyst for the combustion of phthalic anhydride
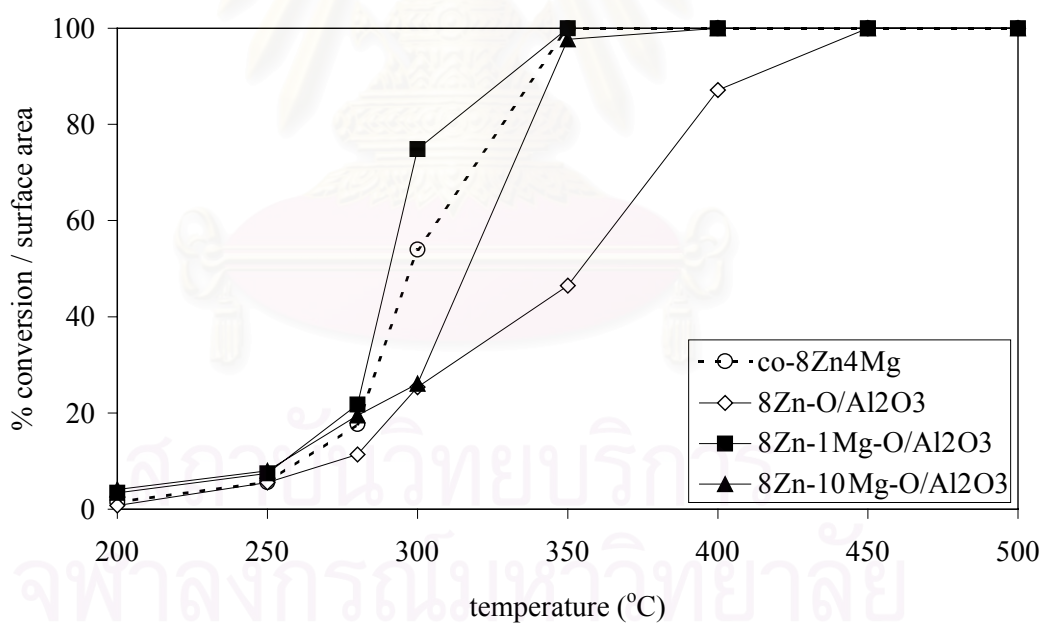
Figure 5.19 The catalytic activity of zinc oxide catalysts base on surface area of catalyst for the combustion of phthalic anhydride
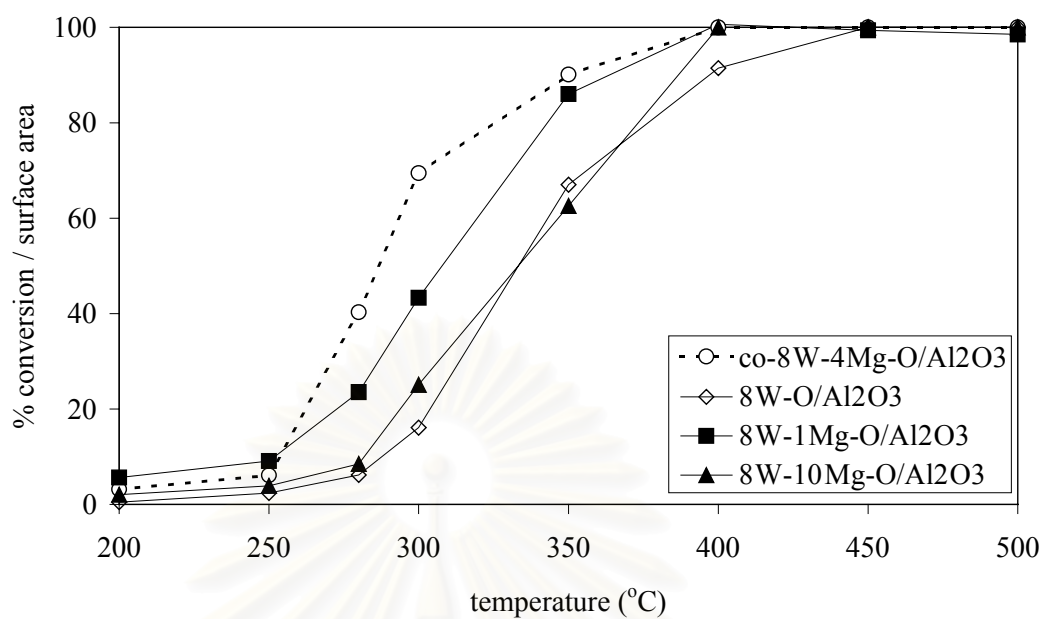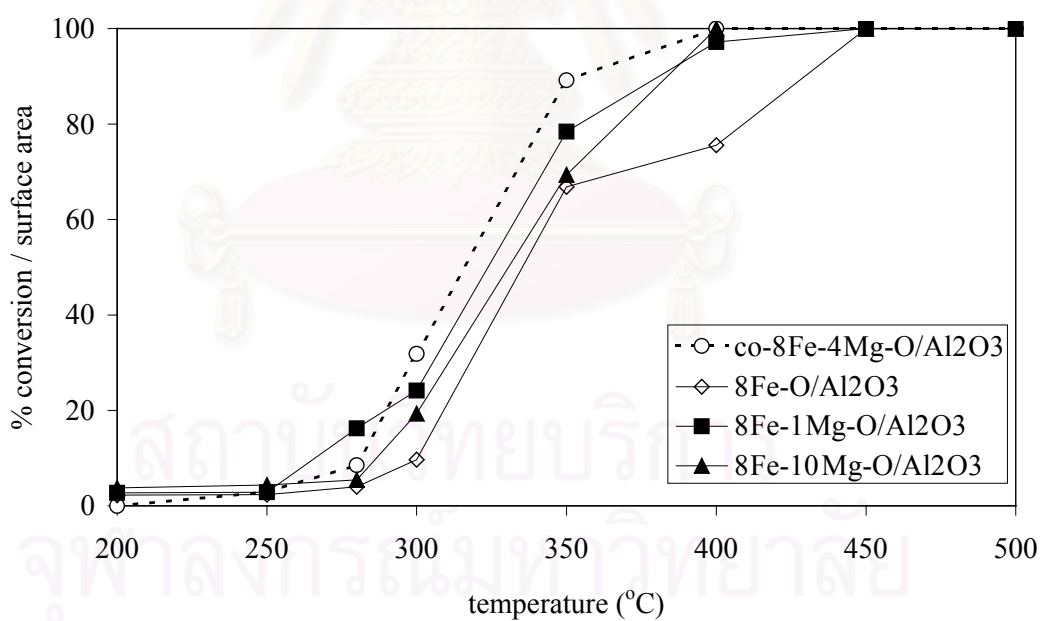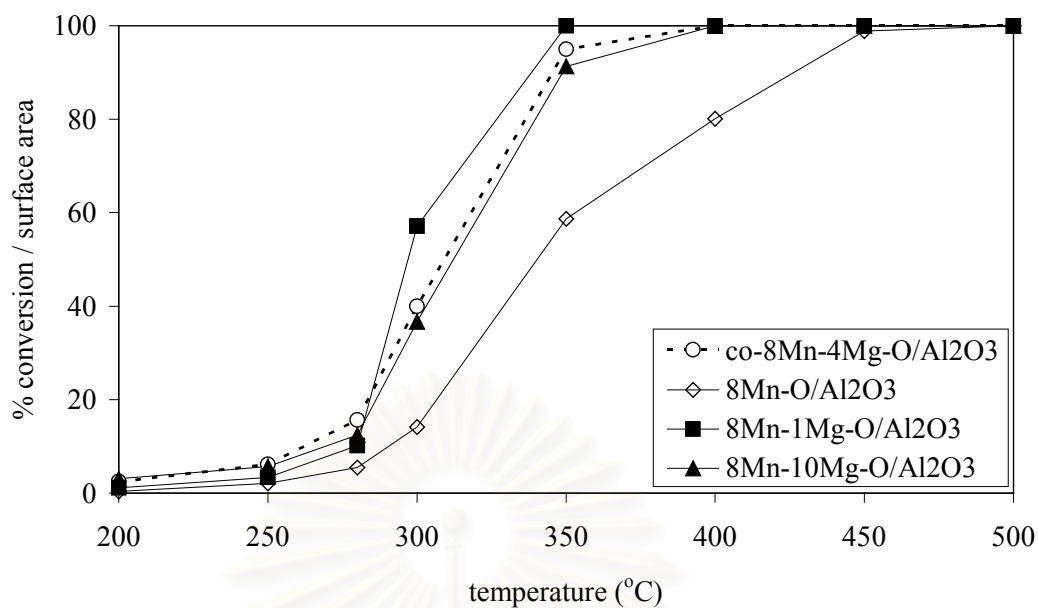
Now let consider the catalyst in group 1. (See Figure 5.20)
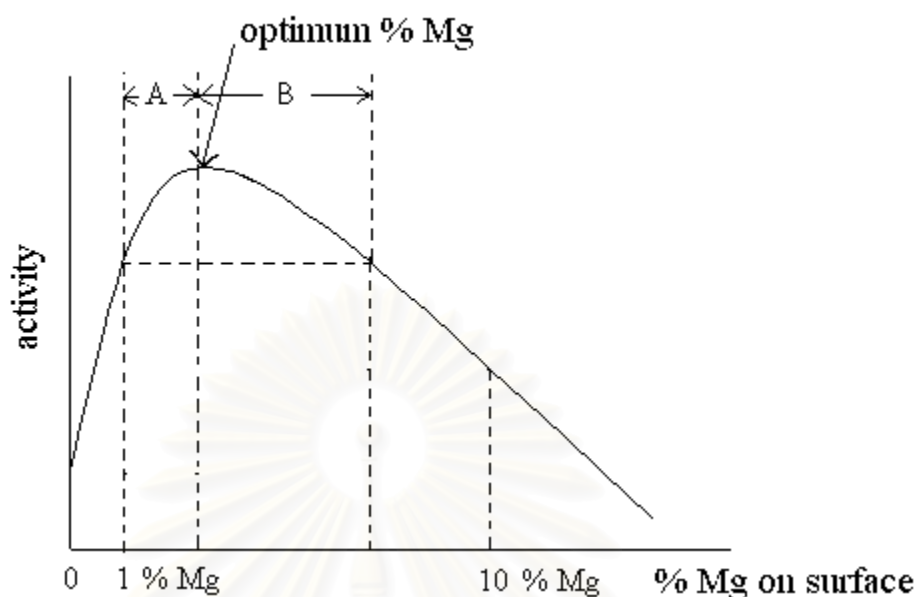
Figure 5.20 The optimum of % magnesium on surface and activity

The catalysts in this group may either fall in regions A or B. If the catalyst falls in region A the more surface basicity would increase the catalytic activity. Catalysts containing tungsten fall in this region. In region B, the more basicity of the surface, the activity decreased. Catalysts containing chromium, molybdenum and iron fall in this region.

The curve of figure 5.20 can be divided into 2 sections as follows

1. 1 wt% to the optimum wt% Mg

This condition is exhibits in Figure 5.21. When the surface basicity increased, the activity increased too. From the hypothesis the results of the tungsten catalysts was likely to be in this range. The tungsten catalysts investigated (4 wt% Mg) in this research had higher activity than 1 wt% Mg. In addition, when the number of the surface basic site increased due to the preparation procedure, the activity increased.

Figure 5.21 The optimum of % magnesium on surface and activity

2. *optimum wt% to A wt% Mg*

This condition is exihibited in Figure 5.22. When the basicity increased, the activity decreased. From the hypothesis, the results of chromium, molybdenum and iron catalysts were likely to be in the range. The chromium, molybdenum and iron catalysts investigated (4 wt% Mg) in this research had higher activity than 1 wt% Mg. However, when the number of the surface basic site increased due to the preparation procedure, the activity decreased.
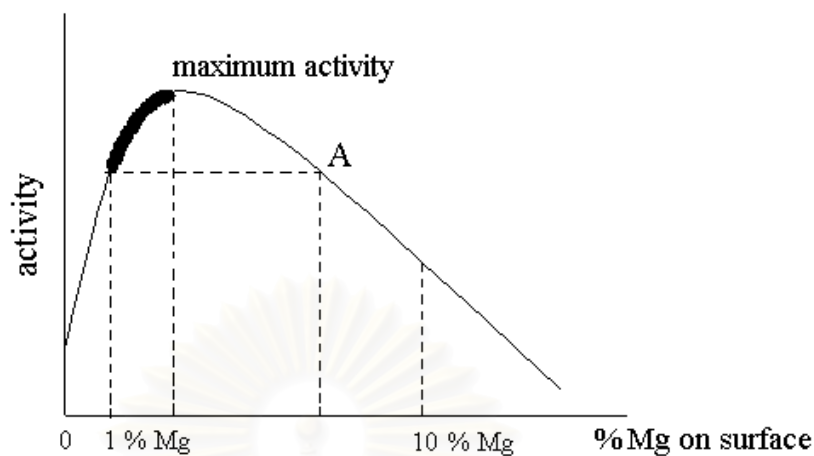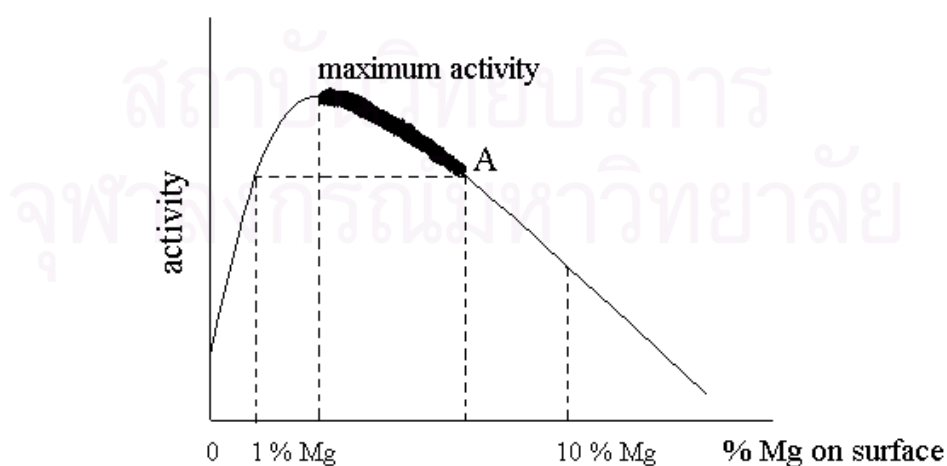

Figure 5.22 The optimum of % magnesium on surface and activity

Next the catalysts in group 2 will be considered. In this region (A wt% to 10 wt% Mg) the more surface basicity the activity decreased

This condition is exhibited in Figure 5.23. When the basicity increased, the activity decreased. From the hypothesis, the results of manganese and zinc catalysts were likely to be in this range. The manganese and zinc catalysts had lower activity than the 1 wt% Mg but still higher than 10 wt% Mg. When wt% Mg was fixed at 4 %, the change in the surface basicity, due to the change in the preparation procedure affects the catalytic activity in the same way i.e. the activity decreased when the surface basicity increased.
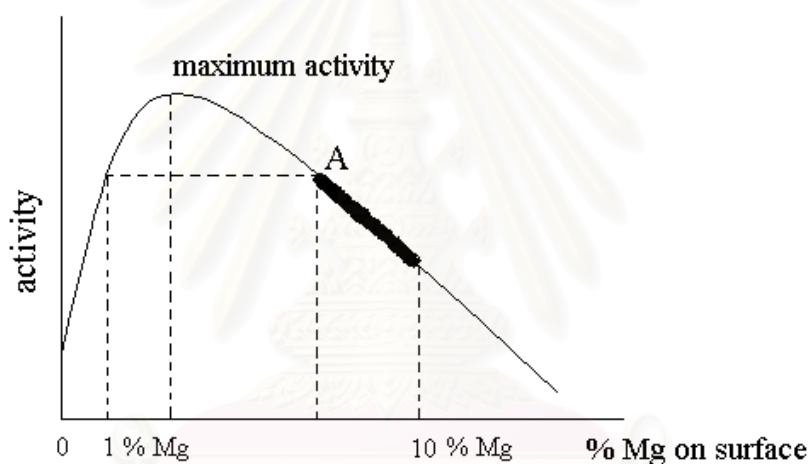
F i g u r e 5.23 The optimum of % magnesium on surface and activity

This research found that the loading sequence of the metal affected the catalytic activity by changing the number of the surface basic sites. The effects would be positive or negative depended on the amount of the magnesium selected. If the amount of magnesium selected was lower than the optimum amount, the procedure that resulted in a large number of the surface basic site would yield a catalyst with higher catalytic activity. On the other hand, if the amount of Mg selected was higher than the optimum amount, the procedure that resulted in a large number of the surface basicity would decrease the catalytic activity.

How the preparation procedure affected the number of the surface basic site is still question, the real structure of the mixed oxide formed in the catalyst could not be

identified due to the limitation and availability of instruments. The transition metals formed new mixed oxides with the magnesium or formed separation transition metal oxides are yet to be founded. Since this formation depends on the transition metal and the ratio of transition metal per magnesium, the scope of the investigative is rather large and is considered to be out of the scope of the present work.

CHAPTER VI

CONCLUSIONS AND RECOMMENDATIONS

6.1 Conclusions

The conclusions of the present research are the following:

1. The sequences of metal loading affected the catalytic activity of Cr-Mg-O/Al$_2$O$_3$, Mn-Mg-O/Al$_2$O$_3$, Mo-Mg-O/Al$_2$O$_3$, W-Mg-O/Al$_2$O$_3$ and Fe-Mg-O/Al$_2$O$_3$ and Zn-Mg-O/Al$_2$O$_3$ catalysts by changing the number of the surface basic sites.

2. The effects of metal loading would be positive or negative depended on the type of transition metal and the amount of the magnesium selected.

3. For phthalic anhydride combustion, magnesium played the role as a promoter for the oxides of Cr, Mn, Mo, W, Fe and Zn catalysts.

6.2 Recommendations for future studies

From the previous conclusions, the following recommendations for future studies can be proposed.

1. Transition metal oxide catalysts were suitable to be used in the catalytic combustion of phthalic anhydride. Therefore, it is interesting to further study the oxidation property of these catalysts with other anhydrides. Such as maleic anhydride which is another organic component exists in some industrial effluent gas.

2. Further study on the structures of the transition metal-Mg-oxides formed on the Al_2O_3 surface to better understand the nature and relationship with their catalytic activity. Some powerful technique such as Electron Spectroscopy for Chemical Analysis (ESCA) (not available in the present work) may be useful for the proposed study.

REFERENCES

Ali, N., Lu, C. and Masel R., "Catalytic oxidaition of odorous oganic acids", *Catalysis Today*, 2000, **62**, 347-353.

Anderson, J.R., and Pratt, K.C*., Introduction to characterization and testing of catalyst*, Sydney, Academic Press, 1985.

Aramendia, M. A., Benitez, J. A., Borau, V., Jimenez, C., Marinas, J. M., Ruiz, J. R. and Urbano, F., "Study of MgO and Pt/MgO systems by XRD, TPR, and H MAS NMR", *Langmuir*, 1999, **15**, 1192-1197.

Bond, G. C., *Heterogeneous Catalysis principles and applications: Chemisorption at oxide surfaces*, Oxford: Clarendon Press, 1987.

Chaiyasit, N., "Application of the Co-Mg-O/TiO_2 catalyst on the selective oxidation of alcohols", *Master's Thesis, Faculty of Engineering, Chulalongkorn University*, 2001.

Cherian, M.; Rao,M.S.; Yang,W.T.; Jehng,J.M.; Hirt, A.M.; and Deo,G., "Oxidative dehydrogenation of propane over Cr_2O_3/Al_2O_3 and Cr_2O_3catalysts : effect of loading, precursor and surface area", *Appl. Catal. A*, 2002, **233**, 21-33.

Hess, K.; Morsbach, B.; Drews, R.; Buechele, W.; and Schachner, H., "Catalyst containing metal oxides for use in the degenerative oxidation of organic compounds present in exhaust gases from combustion plants" *United States Patent*, 1993, **5227356**, 1-20.

Kang, Y.M., and Wan, B.Z., "Effects of acid or base additives on the catalytic combustion activity of chromium and cobalt oxide" *Appl. Catal. A*, 1994, **114**, 35-49.

Keuneche, G., Klopfer, A., and Sterck, L., "Process for continuously separating phthalic anhydride from the reaction gases of the catalytic oxidation of o-xylene and/or naphthalene", *United States Patent*, 1981, **4285871**, 1-22.

Kirk-Othmer. *Encyclopedia of chemical technology: Acidic and Basic catalysts*, John wiley&Sons Inc., 1979.

Larssan,. P.O., and Anderson, A., "Oxides of ceria promoted copper, manganese and copper manganese on Al_2O_3 for the combustion of CO, ethyl acetate and ethanol", *Appl. Catal. B*, 2000, **24**, 175-192.

Leklertsunthorn, R., "Oxidation property of the V-Mg-O/TiO₂ catalyst", *Master's Thesis, Department of Engineering, Graduate School, Chulalongkorn University,* 1998.

Liu, S., Obuchi, A., Uchisawa, J., Nanba, T., and Kushiyama, S., "An exploratory study of diesel soot oxidation with NO₂ and O₂ on supportd metal oxide catalysts", *Appl. Catal. B,* 2002, **37**, 309-319.

McCabe, R.W., and Mitchell, P.J., "Oxidation of Ethanol and Acetaldehyde over Alumina-Supportd Catalysts", *Ind. Eng. Chem. Prod. Res. Dev.,* 1983, **22**, 212-217.

McCarty, J.G., Gusman, M., Lowe, D.M., Hildenbran, D.L., and Lau, K.N., "Stability of supportd metal and Supported metal oxide combustion catalysts", *Catalysis Today,*1999, **47**, 5-17.

Mongkhonsi, T.,Chaiyasit, N., and Praserthdam, P., "Selective Oxidation of 1-Propanol and 2-Propanol over Supported Co-Mg-O Catalysts", *J.Chin.Inst.Chem.Engrs.,* 2002, **33**, 1-8.

Ozkan, U.S., Kueller, R.F., and Moctezuma, E., "Methanol Oxidation over Nonprrecious transition Metal Oxide Catalysts", *Ind. Eng. Chem. Res.,* 1990, **29**, 1136-1142.

Paola,A.D., Lopez, F.G., Ikeda, S., Marci, G., Ohtani, B., and Palmisano, L., "Photocatalytic degradation of organic compounds in aqueous systems by transition metal doped polycrystalline TiO₂", *Catalysis Today,* 2002, **75**, 87-93.

Perry, R.H. and Chilton, C.H., *Chemical Engineering Handbook*, 1973.

Reid, R.C., Pranusnitz, J.M., and Poling, B.E., *The Properties of Gases and Liquids*, McGraw-Hill International Book Company, 1988.

Satterfield, C. N., *Heterogeneous Catalysis in Industrial Practice: Heterogeneous Catalytic Oxidation*, McGraw-Hill, 1980.

Spivey, J.J., "Complete Oxidation of Volatile Organics", *Ind. Eng. Chem.Res.,* 1987, **26**, 2165-2180.

Thammanokul, H., "Oxidative dehydrogenation of propane over V-Mg-O catalysts", *Master's Thesis, Faculty of Engineering, Chulalongkorn University*, 1996.

The JCPDS., *Inorganic Phases Alphabetical Index*, 1980.

Tongsang, P., "The application of V-Mg-O/TiO₂ catalyst on the combustion of anhydrides", *Master's Thesis, Faculty of Engineering, Chulalongkorn University*, 2001.

Toyada, Y.; and Teraji, S., "Process for the treatment of byproducts obtained in the preparation of phthalic anhydride" *United States Patent*, 1980, **4181489**, 1-18.

Umpo, S., "The application of Co-Mg-O/Al$_2$O$_3$ catalyst on the combustion of anhydrides", *Master's Thesis, Faculty of Engineering, Chulalongkorn University*, 2001.

Way, T., and Peter, F., "Apparatus for the recovery of vaporized phthalic anhydride from gas streams" *United States Patent*, 1981, **4252772**, 1-20.

APPENDICES

APPENDIX A

CALCULATION OF CATALYST PREPARATION

Preparation of co-8Cr-4Mg-O/Al$_2$O$_3$ catalysts by the Wet Impregnation Method is shown as follow:

Reagent: - Chromium (III) nitrate nonahydrate [Cr(NO$_3$)$_3$·9H$_2$O]

                Molecular weight = 400.15 g.

              - Magnesium nitrate [Mg(NO$_3$)$_2$]

                Molecular weight = 256.41 g.

Support   - Alumina [Al$_2$O$_3$]

Calculation for the preparation of the 8Cr-4Mg-O/Al$_2$O$_3$ catalyst.

The 8Cr-4Mg-O/Al$_2$O$_3$ aqueous solution used in catalyst preparation consists of Cr 8wt% and Al$_2$O$_3$ 92wt%. The amount of chromium in 8Cr-4Mg-O/Al$_2$O$_3$ catalyst is calculated as follows:

Basis: Al$_2$O$_3$ 1 g

If the weight of catalyst was 100 g, 8Cr-4MgO-/Al$_2$O$_3$ would compose of chromium 8 g and Al$_2$O$_3$ 92 g. Therefore, in this system,

    the amount of Cr   = 8/92 × 1

                                    = 0.0869 g

Chromium (Cr) 0.08695 g was prepared from Cr(NO$_3$)$_3$·9H$_2$O 97% and molecular weight of Cr = 51.996, then

    the Cr(NO$_3$)$_3$·9H$_2$O content   = (400.15×0.08695×100)/(51.996×97)

                                    = 0.6898 g

Then, the Mg: (support + Cr) weight ratio = 4:100

    The amount of Mg   = (0.08695 + 1)×4/100

                                    = 0.0435 g

Magnesium (Mg) 0.0435 g was impregnated from $Mg(NO_3)_2$ solution 99% and molecular weight of Mg = 24.305 g

Thus, the amount of $Mg(NO_3)_2$ used = $(0.0435 \times 256.41 \times 100)/(24.305 \times 99)$

$$= 0.4635 \text{ g}$$

The calculation for the preparation of other catalysts as follow:

co-8Mn-4Mg-O/Al$_2$O$_3$, 8Mn-4Mg-O/Al$_2$O$_3$, 4Mg-8Mn-O/Al$_2$O$_3$, co-8Mo-4Mg-O/Al$_2$O$_3$, 8Mo-4Mg-O/Al$_2$O$_3$, 4Mg-8Mo-O/Al$_2$O$_3$, co-8W-4Mg-O/Al$_2$O$_3$, 8W-4Mg-O/Al$_2$O$_3$, 4Mg-8W-O/Al$_2$O$_3$, co-8Fe-4Mg-O/Al$_2$O$_3$, 8Fe-4Mg-O/Al$_2$O$_3$, 4Mg-8Fe-O/Al$_2$O$_3$, co-8Zn-4Mg-O/Al$_2$O$_3$, 8Zn-4Mg-O/Al$_2$O$_3$, 4Mg-8Zn-O/Al$_2$O$_3$, catalysts were the same as the preparation of co-8Cr-4Mg-O/Al$_2$O$_3$, 8Cr-4Mg-O/Al$_2$O$_3$ and 4Mg-8Cr-O/Al$_2$O$_3$ catalysts.

APPENDIX B

CALCULATION OF DIFFUSIONAL LIMITATION EFFECT

In the present work there are doubt whether the external and internal diffusion limitations interfere with the phthalic anhydride combustion reaction. Hence, the kinetic parameters were calculated based on the experimental data so as to prove the controlled system. The calculation is divided into two parts; one of which is the external diffusion limitation, and the other is the internal diffusion limitation.

1. External diffusion limitation

The phthalic anhydride combustion reaction is considered to be an irreversible first order reaction occurred on the interior pore surface of catalyst particles in a fixed bed reactor. Assume isothermal operation for the reaction.

In the experiment, 0.01% phthalic anhydride, 21% O_2 was used as the unique reactant in the system. Because percentage of phthalic anhydride was rather small compared to the oxygen that it can be neglected. Molecular weight of nitrogen and oxygen are 28.02 and 31.98, respectively. Thus, the average molecular weight of the gas mixture was calculated as follows:

$$M_{AB} = 0.79 \times 28.02 + 0.21 \times 31.98$$
$$= 28.85 \text{ g/mol}$$

Calculation of reactant gas density

Consider the phthalic anhydride combustion is operated at low pressure and high temperature(500°C). We assume that the gases are respect to ideal gas law. The density of such gas mixture reactant at various temperatures is calculated in the following.

$$\rho = PM / RT$$

We obtained : $\rho = 0.455$ kg/m^3

Calculation of the gas mixture viscosity

The simplified methods for determining the viscosity of low pressure binary are described anywhere (Reid, 1988). The method of Wilke is chosen to estimate the gas mixture viscosity.

For a binary system of 1 and 2,

$$\mu_m = \frac{y_1 \mu_1}{y_1 + y_2 \Phi_{12}} + \frac{y_2 \mu_2}{y_2 + y_1 \Phi_{21}}$$

where μ_m = viscosity of the mixture

μ_1, μ_2 = pure component viscosity

y_1, y_2 = mole fractions

$$\phi_{12} = \frac{\left[1 + \left(\dfrac{\mu_1}{\mu_2} \right)^{1/2} \left(\dfrac{M_1}{M_2} \right)^{1/4} \right]^2}{\left[8 \left(1 + \dfrac{M_1}{M_2} \right) \right]^{1/2}}$$

$$\phi_{21} = \phi_{12} \left(\frac{\mu_2}{\mu_1} \right) \left(\frac{M_1}{M_2} \right)$$

M_1, M_2 = molecular weight

Let 1 refer to nitrogen and 2 to oxygen

$M_1 = 28.02$ and $M_2 = 31.98$

From Perry the viscosity of nitrogen at 500°C are 0.0368 cP. The viscosity of oxygen at 500°C are 0.039cP.

$\phi_{12} = 0.971$

$\phi_{21} = 0.902$

$\mu_m = 3.81 \times 10^{-5}$ kg/m-s

Calculation of diffusion coefficients

Diffusion coefficients for binary gas system at low pressure calculated by empirical correlation are proposed by Reid (1988). Wilke and Lee method is chosen to estimate the value of D_{AB} due to the general and reliable method. The empirical correlation is

$$D_{AB} = \frac{\left(3.03 - \frac{0.98}{M_{AB}^{1/2}}\right)\left(10^{-3}\right)T^{3/2}}{PM_{AB}^{1/2}\sigma_{AB}^{2}\Omega_{D}}$$

where D_{AB} = binary diffusion coefficient,cm^2/s

   T   = temperature,K

M_A ,M_B = molecular weights of A and B ,g/mol

$$M_{AB} = 2\left[\left(\frac{1}{M_A}\right)+\left(\frac{1}{M_B}\right)\right]^{-1}$$

   P = pressure,bar

σ = characteristic length,^{0}A

Ω_D = diffusion collision integral, dimensionless

The characteristic Lennard-Jones energy and Length, ε and σ , of nitrogen and oxygen are as follows: (Reid,1988)

For O$_2$: σ = 3.467 ^{0}A, ε/k = 106.7

For N$_2$: σ = 3.798 ^{0}A , ε/k = 71.4

The sample rules are usually employed.

$$\sigma_{AB} = \frac{\sigma_A + \sigma_B}{2} = \frac{3.798 + 3.467}{2} = 3.63$$

$$\varepsilon_{AB}/k = \left(\frac{\varepsilon_A \varepsilon_B}{k^2}\right)^{1/2} = (71.4 \times 106.7)^{1/2} = 87.28$$

Ω_D is tabulated as a function of kT/ε for the Lennard-Jones potential. The accurate relation is

$$\Omega_D = \frac{A}{(T^*)^B} + \frac{C}{\exp(DT^*)} + \frac{E}{\exp(FT^*)} + \frac{G}{\exp(HT^*)}$$

where $T^* = \dfrac{kT}{\varepsilon_{AB}}$, A = 1.06036 , B = 0.15610 , C = 0.19300 , D = 0.47635 , E = 1.03587 , F = 1.52996 , G = 1.76474 , H = 3.89411

Then $T^* = 8.857$

$$\Omega_D = \frac{1.06036}{(T^*)^{0.15610}} + \frac{0.19300}{\exp(0.47635T^*)} + \frac{1.03587}{\exp(1.52996T^*)} + \frac{1.76474}{\exp(3.89411T^*)}$$

$$\Omega_D = 0.757$$

With Equation of D_{AB},

$$D(N_2\text{-}O_2) = 1.123 \text{ m}^2/\text{s}$$

Reactant gas mixture was supplied at 100 ml/min. in tubular microreactor used in the phthalic anhydride oxidation system at 30°C

air flow rate through reactor = 100 ml/min. at 30°C

The density of air , $\rho = 1.161$ kg/m^3

Mass flow rate = 1.935×10^{-6} kg/s

Diameter of stainless steel tube reactor = 9.5 mm

Cross-sectional area of tube reactor $= \dfrac{\pi(9.5\times10^{-3})^2}{4} = 7.09\times10^{-5} \ m^2$

Mass Velocity , $G = 0.027 \ kg/m^2\text{-s}$

Catalyst size $= 40\text{-}60 \ mesh = 0.178\text{-}0.126 \ mm$

Average catalyst size $= (0.126+0.178)/2 = 0.152 \ mm$

Find Reynolds number, Re_p, which is well known as follows:

$$Re_p = \frac{d_p G}{\mu}$$

We obtained

$$Re_p = 0.108$$

Average transport coefficient between the bulk stream and particles surface could be correlated in terms of dimensionless groups, which characterize the flow conditions. For mass transfer the Sherwood number, $k_m\rho/G$, is an empirical function of the Reynolds number, $d_p G/\mu$, and the Schmit number, $\mu/\rho D$. The j-factors are defined as the following functions of the Schmidt number and Sherwood numbers:

$$j_D = \frac{k_m \rho}{G}\left(\frac{a_m}{a_t}\right)(\mu/\rho D)^{2/3}$$

The ratio (a_m/a_t) allows for the possibility that the effective mass-transfer area a_m, may be less than the total external area, a_t, of the particles. For Reynolds number greater than 10, the following relationship between j_D and the Reynolds number well represents available data.

$$\dot{j}_D = \frac{0.458}{\varepsilon_B}\left(\frac{d_p G}{\mu}\right)^{-0.407}$$

where G = mass velocity(superficial) based upon cross-sectional area of empty reactor

$\qquad (G = u\rho)$

d_p = diameter of catalyst particle for spheres

μ = viscosity of fluid

ρ = density of fluid

ε_B = void fraction of the interparticle space (void fraction of the bed)

D = molecular diffusivity of component being transferred

Assume $\varepsilon_B = 0.5$

$j_D = 2.266$

A variation of the fixed bed reactor is an assembly of screens or gauze of catalytic solid over which the reacting fluid flows. Data on mass transfer from single screens has been reported by Gay and Maughan. Their correlation is of the form

$$j_D = (\varepsilon k_m \rho / G)(\mu / \rho D)^{2/3}$$

Where ε is the porosity of the single screen.

Hence, $k_m = (j_D G / \rho)(\mu / \rho D)^{-2/3}$

$$k_m = \left(\frac{0.458G}{\varepsilon_B \rho} \right) Re^{-0.407} Sc^{-2/3}$$

Find Schmidt number, Sc : $Sc = \dfrac{\mu}{\rho D}$

$$Sc = 7.456 \times 10^{-5}$$

Find k_m : $k_m = 75.90$ m/s

Properties of catalyst

Density = 0.375 g/ml catalyst

Diameter of 40-60 mesh catalyst particle = 0.152 mm

Weight per catalyst particle $= \dfrac{\pi(0.152 \times 10^{-1})^3 \times 0.375}{6} = 6.895 \times 10^{-7}$ g/particle

External surface area per particle $= \pi(0.152 \times 10^{-3})^2 = 7.26 \times 10^{-8}$ m^2/particle

a_m $= (7.26 \times 10^{-8})/(6.895 \times 10^{-7}) = 0.105$ m^2/gram catalyst

Volumetric flow rate of gaseous feed stream = 100 ml/min

Molar flow rate of gaseous feed stream = 6.71×10^{-5} mol/s

Phthalic anhydride molar feed rate = $0.0001 \times 6.71 \times 10^{-5} = 6.71 \times 10^{-9}$ mol/s

phthalic anhydride conversion (experimental data): 99.80% at 500°C

The estimated rate of phthalic anhydride oxidation reaction is based on the ideal plug flow reactor which there is no mixing in the direction of flow and complete mixing perpendicular to the direction of flow (i.e., in the radial direction). The rate of reaction will vary with reaction length. Plug flow reactors are normally operated at steady state so that properties at any position are constant with respect to time. The mass balance around plug flow reactor becomes

{rate of i into volume element}- {rate of i out of volume element}

+ {rate of production of i within the volume element}

= {rate of accumulation of i within the volume elecment }

F_{Ao} = $F_{Ao}(1-x) + (r_W W)$

$(r_W W)$ = $F_{Ao} - F_{Ao}(1-x) = F_{Ao} = F_{Ao}x$

r_W = $\dfrac{F_{Ao}x}{W}$ = 6.70×10^{-10} mol/s-gram catalyst

At steady state the external transport rate may be written in terms of the diffusion rate from the bulk gas to the surface. The expression is:

$$R_{obs} = k_m a_m (C_b - C_s)$$

$$= \frac{\text{phthalic anhydride converted (mole)}}{(\text{time})(\text{gram of catalyst})}$$

where C_b and C_s are the concentrations in the bulk gas and at the surface, respectively.

$$(C_b - C_s) = \frac{r_{obs}}{k_m a_m} = 8.407 \times 10^{-11} \text{ mol/m}^3$$

Consider the difference of the bulk and surface concentration is small. It means that the external mass transport has no effect on the phthalic anhydride oxidation reaction rate.

2. Internal diffusion limitation

Next, consider the internal diffusion limitation of the phthalic anhydride reaction. An effectiveness factor, η, was defined in order to express the rate of reaction for the whole catalyst pellet, r_p, in terms of the temperature and concentrations existing at the outer surface as follows:

$$\eta = \frac{\text{actual rate of whole pellet}}{\text{rate evaluated at outer surface conditions}} = \frac{r_p}{r_s}$$

The equation for the local rate (per unit mass of catalyst) may be expected functionally as $r = f(C, T)$.

Where C represents, symbolically, the concentrations of all the involved components

Then, $r_p = \eta r_s = \eta f(C_s, T_s)$

Suppose that the phthalic anhydride oxidation is an irreversible reaction A→B and first order reaction, so that for isothermal conditions $r = f(C_A) = k_1 C_A$. Then $r_p = \eta k_1 (C_A)_s$.

For a spherical pellet, a mass balance over the spherical-shell volume of thickness Δr. At steady state the rate of diffusion into the element less the rate of diffusion out will equal the rate of disappearance of reactant with in the element. This rate will be $\rho_p k_1 C_A$ per unit volume, where ρ_p is the density of the pellet. Hence, the balance may be written, omitting subscript A on C,
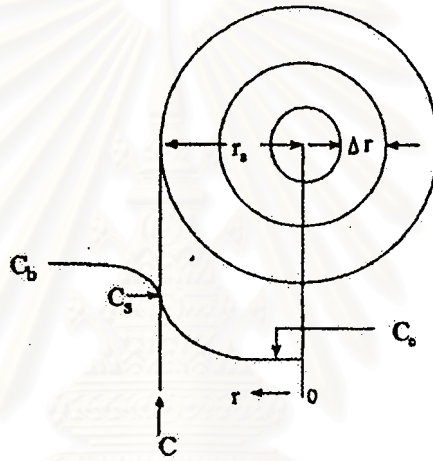

Figure B1. Reactant (A) concentration vs. position for first-order reaction on a spherical catalyst pellet.

$$\left(-4\pi r^2 D_e \frac{dC}{dr} \right)_r - \left(-4\pi r^2 D_e \frac{dC}{dr} \right)_{r+\Delta r} = -4\pi r^2 \, \Delta r_p k_1 C$$

Take the limit as $\Delta r \to 0$ and assume that the effective diffusivity is independent of the concentration of reactant, this difference equation becomes

$$\frac{d^2 C}{dr^2} + 2\frac{dC}{dr} - \frac{k_1 \rho_p C}{D_e} = 0$$

At the center of the pellet symmetry requires

$$\frac{dC}{dr} = 0 \text{ at } r = 0$$

and at outer surface

$$C = C_s \text{ at } r = r_s$$

Solve linear differential equation by conventional methods to yield

$$\frac{C}{C_s} = \frac{r_s \sinh\left(3\phi_s \dfrac{r}{r_s}\right)}{r \sinh 3\phi_s}$$

where ϕ_s is Thiele modulus for a spherical pellet defined by $\phi_s = \dfrac{r_s}{3}\sqrt{\dfrac{k_1 \rho_p}{D_e}}$

Both D_e and k_1 are necessary to use $r_p = \eta k_1 (C_A)_s$. D_e could be obtained from the reduced pore volume equation in case of no tortuosity factor.

$$D_e = (\varepsilon_s^2 D_{AB})$$

$$D_e = (0.5)^2 (1.123) = 0.281$$

Substitute radius of catalyst pellet, $r_s = 7.6 \times 10^{-5}$ m with ϕ_s equation

$$\phi_s = 9.253 \times 10^{-7} \sqrt{k} \text{ (dimensionless)}$$

Find k (at 500°C) from the mass balance equation around plug-flow reactor.

$$r_w = \frac{F_{Ao} \, dx}{dW}$$

where $r_w = kC_A$

Thus, $\qquad kC_A = \dfrac{F_{Ao} \, dx}{dW}$

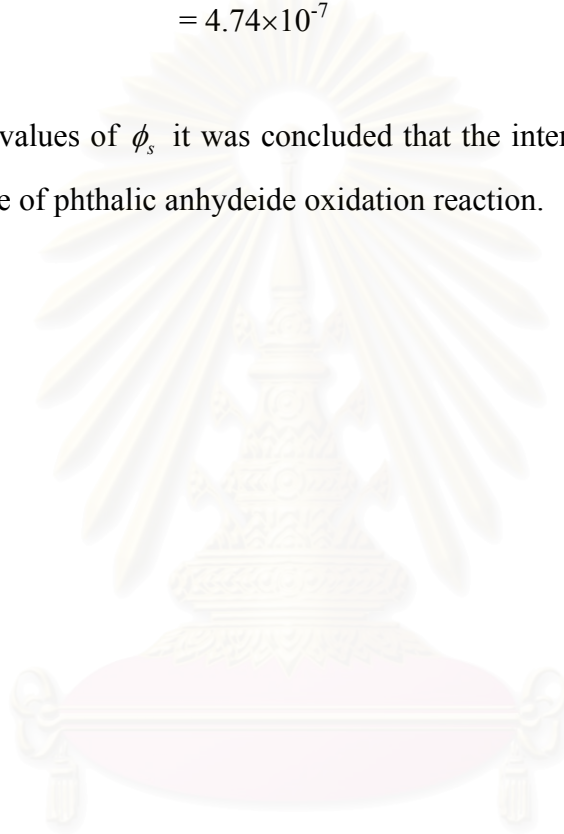$$kC_{Ao}(1\text{-}x) = \frac{F_{Ao}\ dx}{dW}$$

$$W = \frac{F_{Ao}}{kC_{Ao}} \int_{0}^{0.998} \frac{1}{1-x}\ dx$$

$$k = 0.262\ \text{m}^3/\text{s-kg catalyst}$$

Calculate ϕ_s : $\phi_s = 9.253 \times 10^{-7}\ \sqrt{0.262}$

$$= 4.74 \times 10^{-7}$$

For such small values of ϕ_s it was concluded that the internal mass transport has no effect on the rate of phthalic anhydeide oxidation reaction.

APPENDIX C

CALCULATION OF SPECIFIC SURFACE AREA

From Brunauer-Emmett-Teller (BET) equation [Anderson and co-worker (1985)]

$$\frac{p}{n(1-p)} = \frac{1}{n_m C} + \frac{(C-1)p}{n_m C} \tag{C1}$$

Where, p = Relative partial pressure of adsorbed gas, P/P_0

P_0 = Saturated vapor pressure of adsorbed gas in the condensed state at the experimental temperature, atm

P = Equilibrium vapor pressure of adsorbed gas, atm

n = Gas adsorbed at pressure P, ml. at the NTP/g of sample

n_m = Gas adsorbed at monolayer, ml. at the NTP/g of sample

C = Exp $[(H_C - H_l)/RT]$

H_C = Heat of condensation of adsorbed gas on all other layers

H_l = Heat of adsorption into the first layer

For the single point method, the graph must pass through the origin. Therefore, the value of C must be assumed to be infinity.

$C \rightarrow \infty$, then equation C1 is reduced to

$$\frac{p}{n(1-p)} = \frac{p}{n_m}$$

$$n_m = n(1-p) \tag{C2}$$

The surface area, S, of the catalyst is given by

$$S = S_b \times n_m \tag{C3}$$

From the gas law

$$\frac{P_b V}{T_b} = \frac{P_t V}{T_t} \tag{C4}$$

Where, P_b = Pressure at 0ºC

P_t = Pressure at tºC

T_b = Temperature at 0ºC = 273.15 K

T_t = Temperature at t°C = 273.15 + t K

V = Constant volume

Then, P_b = (273.15/ T_t) × P_t = 1 atm

Partial pressure

$$P = \frac{\left[\text{Flow of } (He + N_2) - \text{Flow of He}\right]}{\text{Flow of } (He + N_2)} \qquad (C5)$$

= 0.3 atm

For nitrogen gas, the saturated vapor pressure equals to

P_0 = 1.1 atm

then, p = P/P_0 = 0.3/1.1 = 0.2727

To measure the volume of nitrogen adsorbed, n

S_1

S_2

N_2 1 ml/1 atm at room   Desorption of N_2 area
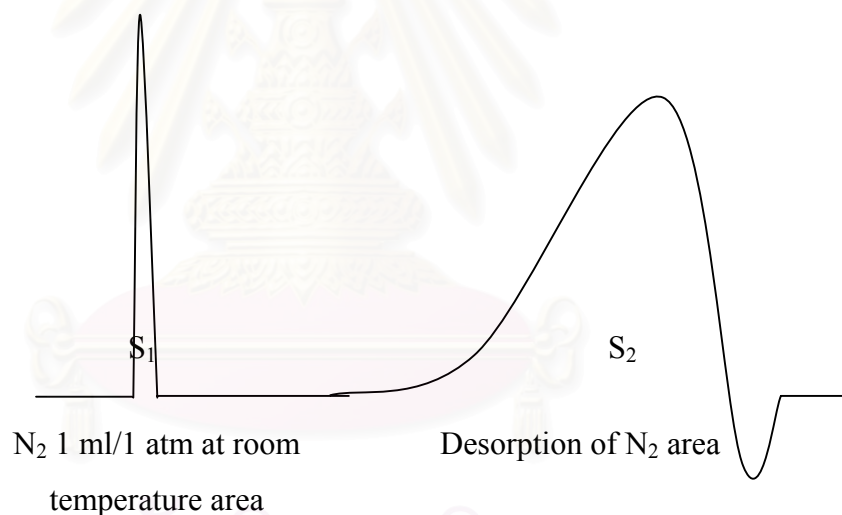
temperature area

$$n = \frac{S_2}{S_1} \times \frac{1}{W} \times \frac{273.15}{T} \text{ ml/g of catalyst} \qquad (C6)$$

Where, S_1 = N_2 1 ml/1 atm at room temperature area

S_2 = Desorption of N_2 area

W = Sample weight, g

T = Room temperature, K

Therefore,

$$n_m = \frac{S_2}{S_1} \times \frac{1}{W} \times \frac{273.15}{T} \times (1-p)$$

$$n_m = \frac{S_2}{S_1} \times \frac{1}{W} \times \frac{273.15}{T} \times 0.7272 \qquad (C2.1)$$

Whereas, the surface area of nitrogen gas from literature equal to

$$S_b = 4.373 \ m^2/ml \ of \ nitrogen \ gas$$

Then,

$$S = \frac{S_2}{S_1} \times \frac{1}{W} \times \frac{273.15}{T} \times 0.7272 \times 4.343$$

$$S = \frac{S_2}{S_1} \times \frac{1}{W} \times \frac{273.15}{T} \times 3.1582 \ m^2/g \qquad (C7)$$

APPENDIX D

CALIBRATION CURVE

Flame ionization detector gas chromatographs Shimadzu model 9A equipped with a Chromosorb WAW column is used to analyze the concentrations of phthalic anhydride, maleic anhydride, acetic acid, ethylbenzene, toluene, and benzene.

The Porapak-Q and Molecular Sieve 5-A column are used with a gas chromatograph equipped with a thermal conductivity detector, Shimadzu model 8A, to analyze the concentration of CO_2 and CO.

The calibration curves of phthalic anhydride and carbon dioxide are illustrated in the following figures.
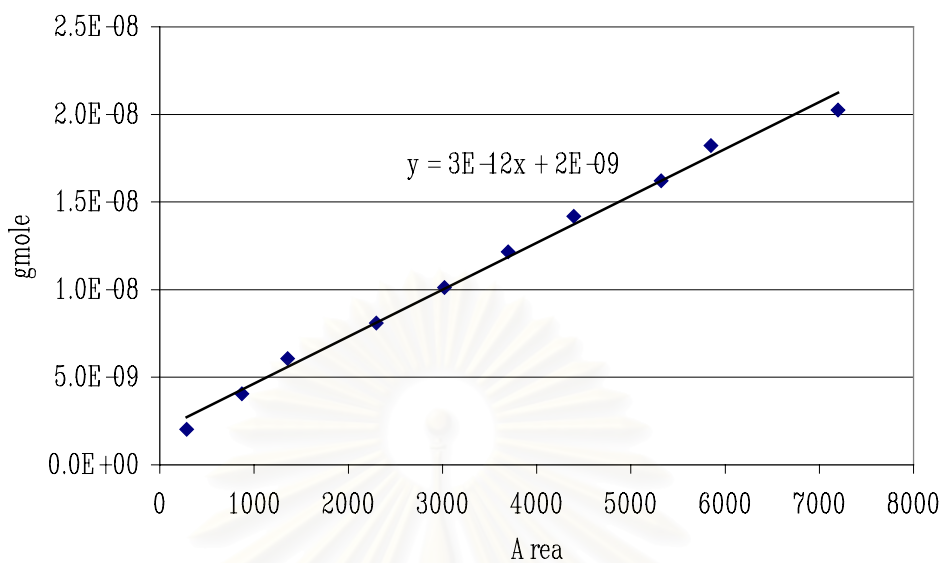
Figure D1 The calibration curve of phthalic anhydride
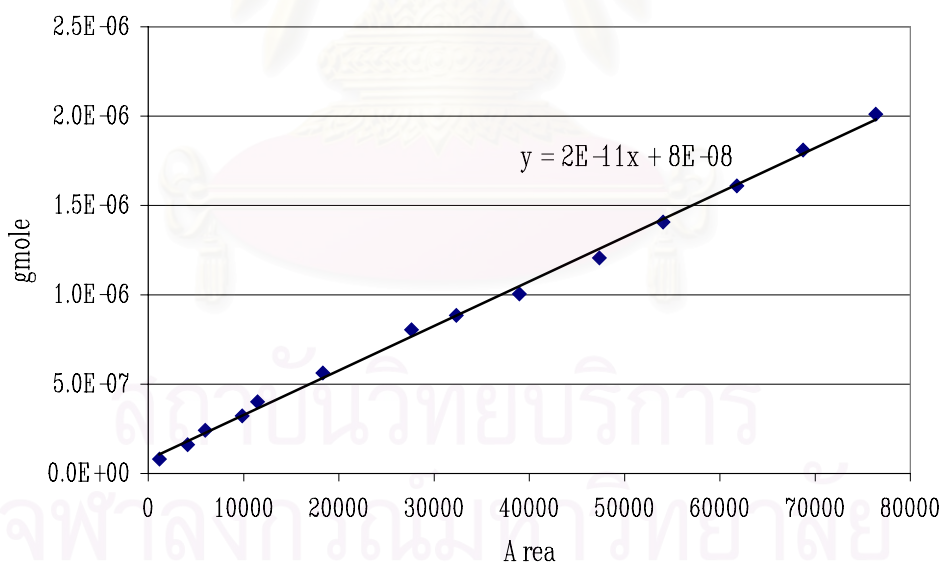

Figure D2 The calibration curve of carbon dioxide

APPENDIX E

DATA OF EXPERIMENTS

Table E1 Data of Figure 5.7

Temp (°C)	Phthalic anhydride conversion (%)		
	co-8Cr-4Mg-O/Al$_2$O$_3$	8Cr-4Mg-O/ Al$_2$O$_3$	4Mg-8Cr-O/Al$_2$O$_3$
200	9.65	8.67	6.59
250	22.74	23.09	23.34
280	35.85	33.38	30.00
300	67.45	68.70	69.77
350	93.00	86.92	87.00
400	98.00	97.72	96.00
450	100.00	98.76	97.95
500	100.00	100.00	100.00

Table E2 Data of Figure 5.8

Temp (°C)	Phthalic anhydride conversion (%)		
	co-8Mn-4Mg-O/Al$_2$O$_3$	8Mn-4Mg-O/Al$_2$O$_3$	4Mg-8Mn-O/Al$_2$O$_3$
200	2.11	1.30	2.70
250	5.18	3.19	10.08
280	13.12	6.99	15.00
300	17.16	10.56	22.00
350	69.00	72.93	80.87
400	91.34	90.00	88.00
450	98.00	99.00	97.00
500	100.00	99.88	100.00

Table E3 Data of Figure 5.9

Temp (°C)	Phthalic anhydride conversion (%)		
	co-8Mo-4Mg-O/Al$_2$O$_3$	8Mo-4Mg-O/Al$_2$O$_3$	4Mg-8Mo-O/Al$_2$O$_3$
200	1.11	1.80	1.87
250	2.56	2.76	2.28
280	2.64	3.62	2.79
300	38.44	25.94	18.67
350	84.85	82.71	85.33
400	92.69	93.73	93.73
450	99.00	100.00	100.00
500	100.00	100.00	100.00

Table E4 Data of Figure 5.10

Temp (°C)	Phthalic anhydride conversion (%)		
	co-8W-4Mg-O/Al$_2$O$_3$	8W-4Mg-O/Al$_2$O$_3$	4Mg-8W-O/Al$_2$O$_3$
200	3.01	1.41	1.03
250	5.81	4.00	2.83
280	38.19	31.47	34.79
300	65.80	56.11	60.00
350	85.39	85.39	84.73
400	99.00	97.00	93.49
450	100.00	100.90	99.15
500	100.00	100.00	100.00

Table E5 Data of Figure 5.11

Temp (°C)	Phthalic anhydride conversion (%)		
	co-8Fe-4Mg-O/Al$_2$O$_3$	8Fe-4Mg-O/Al$_2$O$_3$	4Mg-8Fe-O/Al$_2$O$_3$
200	0.00	0.48	0.55
250	2.28	4.63	2.38
280	6.67	7.14	7.098
300	24.8	23.91	29.64
350	69.63	71.00	73.56
400	94.33	92.00	91.08
450	99.06	100.00	100.00
500	100.00	100.00	100.00

Table E6 Data of Figure 5.12

Temp (°C)	Phthalic anhydride conversion (%)		
	co-8Zn-4Mg-O/Al$_2$O$_3$	8Zn-4Mg-O/Al$_2$O$_3$	4Mg-8Zn-O/Al$_2$O$_3$
200	1.17	0.37	1.79
250	4.54	3.69	4.92
280	14.26	10.07	14.64
300	43.49	33.07	21.37
350	89.92	78.85	62.01
400	100.00	100.00	100.00
450	100.00	100.00	100.00
500	100.00	100.00	100.00

Table E7 Data of pyridine and maleic anhydride adsorption of Table 5.3 to 5.8

catalyst	Pyridine	maleic
Al2O3	86,019	2,099
co-8Cr-4Mg-O/Al$_2$O$_3$	78,409	2,770
8Cr-4Mg-O/Al$_2$O$_3$	78,857	2,686
4Mg-8Cr-O/Al$_2$O$_3$	79,137	2,623
co-8Mn-4Mg-O/Al$_2$O$_3$	136,922	2,204
8Mn-4Mg-O/Al$_2$O$_3$	134,844	2,267
4Mg-8Mn-O/Al$_2$O$_3$	138,007	2,161
co--8Mo-4Mg-O/Al$_2$O$_3$	143,145	1,574
8Mo-4Mg-O/Al$_2$O$_3$	138,079	1,637
4Mg-8Mo-O/Al$_2$O$_3$	135,687	1,679
co-8W-4Mg-O/Al$_2$O$_3$	134,872	3,100
8W-4Mg-O/Al$_2$O$_3$	133,374	3,167
4Mg-8W-O/Al$_2$O$_3$	129,585	3,241
co-8Fe-4Mg-O/Al$_2$O$_3$	47,291	3,568
8Fe-4Mg-O/Al$_2$O$_3$	47,544	3,547
4Mg-8Fe-O/Al$_2$O$_3$	51,781	3,463
co-8Zn-4Mg-O/Al$_2$O$_3$	51,143	3,002
8Zn-4Mg-O/Al$_2$O$_3$	49,879	3,090
4Mg-8Zn-O/Al$_2$O$_3$	50,544	3,167

APPENDIX F

MATERIAL SAFETY DATA SHEETS OF

PHTHALIC ANHYDRIDE

Safety data for phthalic anhydride

General

Synonyms: 1,2-benzenedicarboxylic acid anhydride, phthalic acid anhydride
Molecular formula: $C_8H_4O_3$

Physical data

Appearance: white crystalline solid with choking odour
Melting point: 131°C
Boiling point: 295°C
Vapour density: 5.1 (air=1)
Density (g cm^{-1}): 1.53
Flash point: 152°C (closed cup)
Explosion limit: 1.7-10.5%
Water solubility: slight

Stability

Stable. Combustible. Incompatible with strong oxidizing agents, strong bases, moisture, nitric acid, alkalies. Dust may form an explosive mixture with air.

Toxicology

Corrosive - causes burns. Harmful if swallowed or inhaled. Skin or eye contact may cause severe irritation. Typical TLV/TWA 1 ppm. Typical STEL 4 ppm. Typical PEL 2 ppm.

Personal protection

Safety glasses, gloves, adequate ventilation.

APPENDIX G
PROCEDURE AND CALCULATION OF PYRIDINE AND
MALEIC ANHYDRIDE ADSORPTION

Pyridine Adsorption

The nitrogen gas flowed through the system that consisted of a tube connected to the gas chromatograph (GC9A). The sample was placed in the tube as shown in Figure G1.
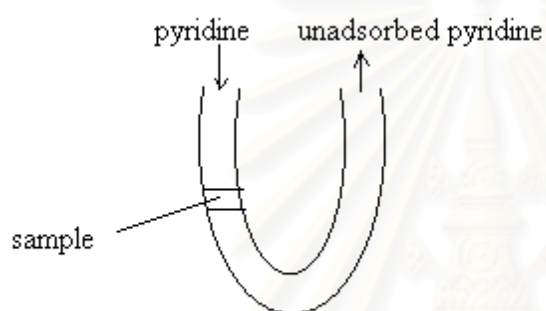

Figure G1 The adsorption system

The pyridine was injected into the column. The sample would adsorb a part of the pyridine. The pyridine that was not adsorbed on the sample was measured by the gas chromatograph. The pyridine was injected until the peaks were constant. It meant that the sample was saturated with pyridine.

The peaks of the unadsorbed pyridine that were detected from the gas chromatograph were shown in Figure G2.
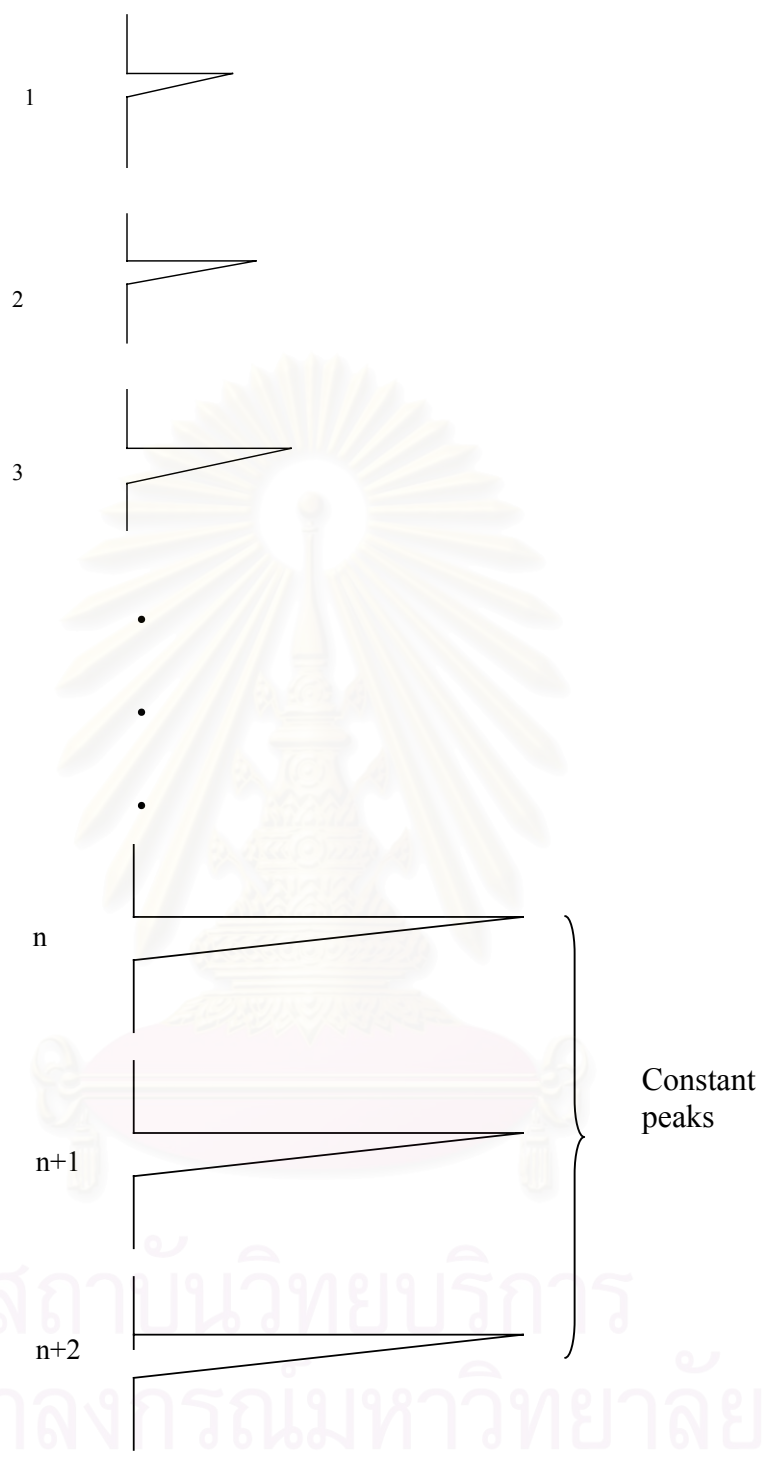
Figure G2 The unadsorbed pyridine peaks

The overall pyridine adsorbed was calculated by subtraction the area of constant peaks with the 1st peak, 2nd peak, …, respectively. The summation of these subtracted areas was the overall area of the pyridine adsorbed.

$$\text{Overall pyridine adsorbed} = \sum (\text{area of constant peak} - \text{area of peak}_i)$$

Maleic anhydride adsorption

The procedure of the maleic anhydride adsorption was the same as the procedure of the pyridine adsorption but the pyridine injection was changed to the maleic anhydride injection. An aqueous solution of maleic anhydride (0.104 g/ml) was used.
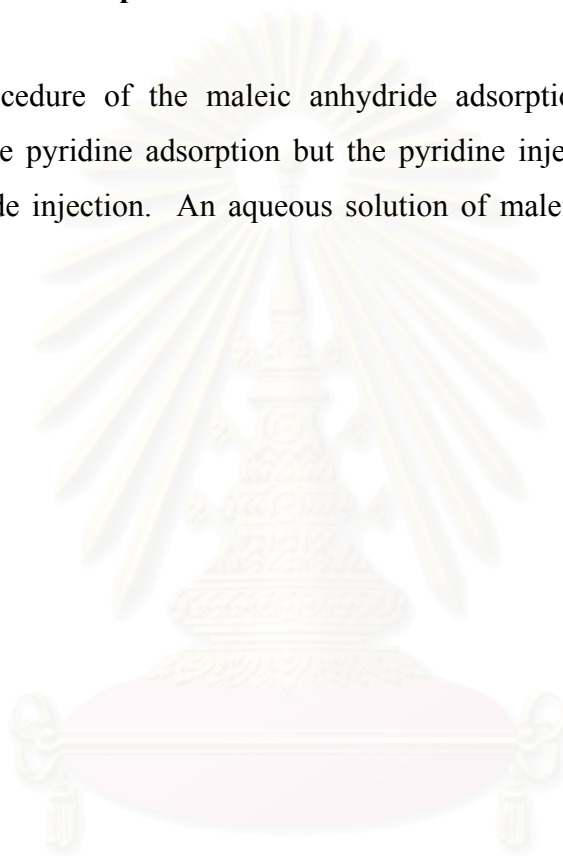
VITA

Miss Suteera Nuampituk was born on December 20th, 1978 in Bangkok, Thailand. She received the Bachelor Degree of Chemical Engineering from Faculty of Engineering, Kasetsart University in 2001. She continued her Master's Study at Chulalongkorn University in June, 2001.